

Original Research

View Article Online



Received 03 August 2022

Revised 31 August 2022

Accepted 31 August 2022

Available online 21 September 2022

Edited by Shafi Ullah Khan

KEYWORDS:

SARS-CoV-2

Moringa oleifera

beta carotene

myricetin

Drum stick plant

Natr Resour Human Health 2023; 3 (1): 101-126

<https://doi.org/10.53365/nrfhh/153401>

eISSN: 2583-1194

Copyright © 2023 Visagaa Publishing House

In silico Investigation of inhibitory characteristics of phytoconstituents from *Moringa oleifera* against SARS-CoV-2 viral proteins

Amit Kumar Shrivastava^{1,*}, Dipendra Chaudhary², Laxmi Shrestha¹, Anjan Palikhey¹, Chandrajeet Kumar Yaadav¹, Deepak Basyal³, Bishal Joshi⁴, Mohammad Ujair Shekh⁵

¹Department of Pharmacology, Universal College of Medical Sciences, Bhairahawa, Rupandehi, Nepal

²Department of Pharmacy, Lumbini Provincial Hospital, Butwal, Rupandehi, Nepal

³Department of Pharmacy, Maharajgunj Medical Campus, Institute of Medicine, Tribhuvan University, Nepal

⁴Department of Physiology, Universal College of Medical Sciences, Bhairahawa, Rupandehi, Nepal

⁵Department of Pharmacy, Universal College of Medical Sciences, Bhairahawa, Rupandehi, Nepal

ABSTRACT: The global pandemic situation caused by rare viral pneumonia occurs in late December 2019 in Wuhan, China, which we now recognize as COVID-19. The molecular docking was used to identify potential phytoconstituents of *Moringa oleifera* and reference drug hydroxychloroquine on SARS-CoV-2 main protein by using AutoDock 4.2.6 and Auto dock Vina. All the physicochemical and bioactive parameters (ADME, toxicity study, receptor interaction, PASS analysis, drug-likeness) were determined using different online validated software. The binding energy of all SAR-CoV-2 proteins with selected phytoconstituents of *Moringa oleifera* were found to be beta carotene, vitamin E; myricetin, quercetin showed the highest binding affinity with all interacting proteins comparable with other drugs and reference drug hydroxychloroquine as an order: beta carotene > myricetin > quercetin > vitamin E > hydroxychloroquine > quinic acid. The MD simulation analysis of viral protein (6MOJ) with beta carotene, vitamin E and myricetin demonstrated strong stability at 300 K. All three complexes exhibit persistent RMSDs value (0.25 – 1.5 Å) of protein side-chain C α atoms during the 3 ns MD simulation time scale. The minor changes of all three ligands with 2 different viral proteins increasing the compactness of ligands with protein in radius of gyration suggested the strong structural activity of ligands and the least fluctuation during the MD simulation (31.2, 30.0 and 31.2), respectively. In the present study revealed that all the active constituents of *Moringa oleifera* show good binding affinity, but beta carotene and myricetin have an excellent affinity with SARS-CoV-2 proteins respectively.

1. INTRODUCTION

Severe Acute Respiratory Syndrome Coronavirus 2 (SARS-CoV-2) enter the host cell through the Endosomal pathway. The mechanism of SARS-CoV-2 replication into the host cell is represented in Figure S1, Appendix A. The viral spike protein binds to the cellular cell surface receptor angiotensin-converting enzyme 2 (ACE 2) and form the ACE-2 virus complex, then translocated to the endosome into the cell. The spike protein is cleaved by the Endosomal acid proteases and activate Endosomal viral entry. The virus that has been internalized

loses its coating, allowing the viral DNA to enter the cytoplasm. The SARS-CoV-2 viral RNA is replicated and translated; after that, the viral RNA encodes the structural components such as spike, nucleocapsid, and membrane and envelope protein into the endoplasmic reticulum. The development of this vital component assembled the viral genome and released the virus via vascular endocytosis (Ang et al., 2020; Du et al., 2009; Murgolo et al., 2021).

Treatment for SERS and MERS infection is still available, but for COVID-19, there is no proven antiviral drugs are available, still the COVID-19 vaccines are available which

* Corresponding author.

E-mail address: sr.akshri.ucms.np@gmail.com (Amit Kumar Shrivastava)

This is an open access article under the CC BY-NC-ND license (<http://creativecommons.org/licenses/by-nc-nd/4.0/>).

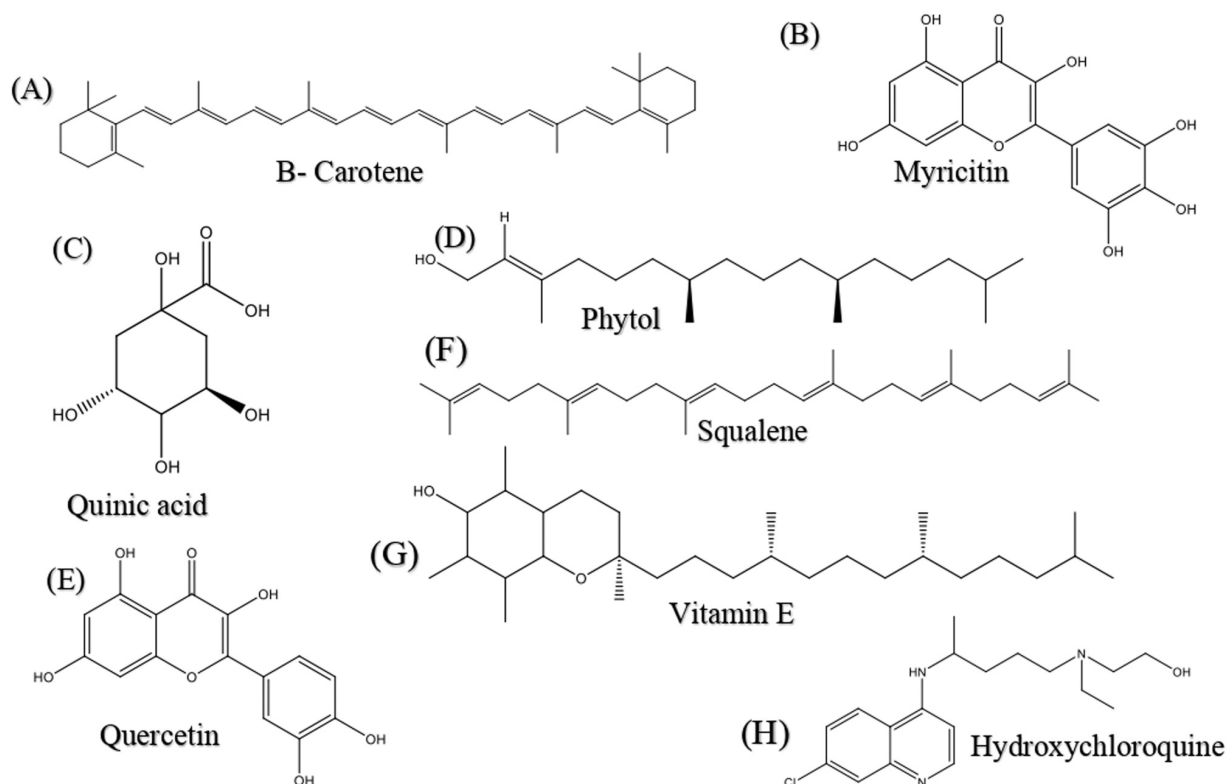


Figure 1. Chemical structure of active phyto-constituent of *Moringa oleifera* used in this study (A) beta carotene, (B) Myricetin, (C) Quinic acid, (D) Phytol, (E) Quercetin, (F) Squalene, (G) Squalene and (H) Hydroxychloroquine.

is capable to reduce the mortality rate. Initial therapy of suspected COVID-19 patients is to be isolated for preventing cross-contamination, supportive care like oxygen therapy, fluid management, and some antibiotics are recommended for the management of secondary infection. The COVID-19 patients are rapidly progressed to acute respiratory distress syndrome (ARDS) and septic shock (Harapan et al., 2020). The gradual increases of viral infection and death of the peoples many researchers searching for the alternative way for the management of this disease and stimulate the immune system. Therefore, researchers looking for ancient scriptures like Ayurveda, Unani etc. to find out the herbs and their constituents for the management of COVID-19 infection. Natural remedies (herbal medicine) were crucial in the treatment of infectious diseases in the past (Ang et al., 2020). The existing reports and evidence are not possible to completely deny to use of food and herbal medicine or remedies as a complementary therapy for the prevention of infection, maintaining immunity. Previously Panyod et al. (2020) and Yang et al. (2020) was summarized the many herbal medicines are used for

the management of COVID-19 infection and improve the associated complications into the patients. This study will evaluate the effect of *Moringa oleifera* containing phyto-constituents on SARS-CoV-2 proteins.

The *Moringa oleifera*, a member of the *Moringaceae* family, is also known as the Drumstick tree or horseradish tree. This plant is commonly found in the sub-Himalayan region of Northern India, Bangladesh, Nepal, and Pakistan. The tropical and sub-tropical region of this plant is suitable for cultivation. *Moringa oleifera* is commonly referred to as “Miracle Tree” because of their nutritional values (Thapa et al., 2019). The *Moringa oleifera* is used as anti-inflammatory, antioxidant, antihypertensive, immunomodulatory, antimicrobial, and upregulation of TNF- α activities etc. (Alegbeleye, 2018). In this pandemic situation, people are interested in exploring medicinal plants with a potential active constituent that counters the infection and maintains the immune system. Thus, some specific plants have excellent potential to show antiviral activity and support the immune system, the *Moringa*

oleifera in one of them. In the present study through *in-silico* approach, try to include some active constituents of *Moringa oleifera* according to their potential therapeutic value, which was not used previously to identify compounds' efficacy properly. The molecular docking and Molecular dynamic simulation analysis is a computational tool used to determine ligand's effect with different structural proteins. It represents the actual behaviour of ligand with proteins and helps to screen the actual affinity of new compounds. This method was rapid, less time-consuming, and provides sufficient information regarding the new compounds for drug discovery. With the help of this method, we can easily determine the effect of unknown compounds with specific protein/receptor interaction. The MD simulation is a validation tool of molecular docking. This analysis selected the highest binding affinity. The ligand protein complexes are further identified the stability with proteins in biological system-like behaviour.

2. MATERIAL AND METHODS

2.1. Drug and ligand preparation

The present study was done in the cheminformatics section of pharmacology department, Universal College of Medical Sciences, Bhairahawa, Rupandehi, Nepal, from December 2021 to June 2022. A total of seven phyto-constituents of *Moringa Oleifera* (Drumstick) were selected from Dr. Duke's phytochemical and ethnobotanical databank (<https://phytochem.nal.usda.gov/phytochem/search/list>). The compounds were selected based on activity and their presence at high concentrations. The compounds used in present study were β - carotene (PCID 5280489), myricetin (PCID 5281672), phytol (PCID 5280435), quinic acid (PCID 6508), quercetin (PCID 5280343), squalene (PCID 638072), vitamin E (PCID 14985) and hydroxychloroquine (PCID 9579) were obtained from PubChem database (<https://pubchem.ncbi.nlm.nih.gov/>) in SDF format (Figure 1). The ligand was prepared, and energy minimization was done through Merck molecular force field (MMFF94) Chem draw office 17.1 version. The hydroxychloroquine (HCQ) have good inhibitory action against SARS-CoV-2 viral proteins, and various clinical trials were conducted. Thus, in the present study HCQ was used as a standard compound. All the data ware indicated that HQC was effective in COVID-19 infection and shows mild adverse effects (Touret & De Lamballerie, 2020).

2.2. Prediction of activity spectra for substances (PASS) analysis

The ligand protein interaction studies have been conducted in both dry and wet lab for the drug discovery through computational system and molecular approach. It helps to define the specificity and affinity of drugs with macromolecules (Feng et al., 2017). The conventional experimental approach is complicated, time-consuming, and expensive for determining drug target interactions. In recent years a computational approach receives the intension of many research for the identification of drug target interaction. Through this method accurately define the drug affinity with target (Li et al., 2021).

The PASS analysis is the online program was used for biological actions of a drug compound based on the structure-activity relationship (SAR) with known compounds. The present study used various online and offline tools such as Lipinski's rule of five (calculate $MW \leq 500$, $\log P \leq 5$, number of hydrogen bond donors (NOHNH) ≤ 5 and hydrogen bond acceptor (NON) ≤ 10 , topological polar surface area (TPSA) $\leq 140 \text{ \AA}$ and number of rotational bond (≤ 10) (Lipinski et al., 1997). Ghose filter determines the receptor binding affinity, cellular uptake, drug bioavailability which was highly influenced of drug Lipophilicity and molar refractivity, the compounds are active in 3D- QSAR studies to evaluate the drug like character (Lipinski et al., 1997). Based on the structure-activity relationship (SAR), the study was carried out using OSIRIS Property Explorer version 4.5.1 (<http://www.openmolecules.org/propertyexplorer/index.html>) to identify the biological, pharmacological, and mechanism of action of molecules (Ahmad, 2019; Dolinsky et al., 2007; Faber et al., 2005; Fang et al., 2003; Ferriola et al., 1989; Franova et al., 2016; Gupta et al., 2021).

2.3. Drug likeness prediction

OSIRIS property explorer predicted drug-likeness was used for chemical structure and determination of various drug-related properties, including TPSA, clog P, molecular weight, hydrogen bond donor, nitrogen and hydrogen atoms and drug score. The only difference from PASS analysis is the number of violations for orally active phytoconstituents is limited to one. The Lipinski's rule five helps to evaluate pharmacokinetic and molecular properties of active compounds (Egan et al., 2000; Ghose et al., 1999; Lipinski et al., 1997; Muegge et al., 2001; Veber et al., 2002).

2.4. Bioactivity score prediction (BAS)

The bioactivity score of all compounds were predicted using an online tool (Molispiration version 2016.10) concerning SARS-CoV-2 selected proteins. The drug score helps to determine the potential effect of bioactive compounds. The BAS rule states that a drug is physiologically active if it is >0.0 , moderately active if it is between -5.0 and 0.0 , and inactive if it is <-5.0 . Additionally, the number of rotational bonds, H-bond acceptors, and H-bond donors were calculated using BAS tool (Ahmad, 2019; Martin, 2005; Verma, 2012).

2.5. Pharmacokinetic (ADME) prediction

The ADMET analysis of compound deals with absorption, distribution, metabolism, excretion, and toxicity in humans. There are lots of online and offline software available to determine pharmacokinetic parameters (ADMET). In the present study, SwissADMEs online tools was used for the prediction of behaviour of the drug candidates (Ahmad, 2019).

2.6. Brain and Gastrointestinal Estimated Permeation Analysis (BOILED-Egg)

The blood-brain barrier permeability and gastrointestinal (GI) absorption are crucial pharmacokinetics parameters to assess the action of certain novel compounds. These two parameters are accessed through the Brain and Intestinal EstimateD Permeation (BOILED-Egg) model by using SwissADME software in which all the active phytoconstituents of *Moringa oleifera* and hydroxychloroquine were subjected to lipophilicity (WLOGP) and polarity (TPSA) computation (Gupta et al., 2021).

2.7. Bioavailability radar

The bioavailability radar, also known as the "spider" plot, virtually it describes a molecules drug-likeness. The pink colour zone represents oral bioavailability, and to be considered a drug-like molecule, the molecule radar must occur entirely within the radar zone. Lipophilicity, scale, polarity, solubility, versatility, and saturation are six physicochemical properties were found in the pink region (Gupta et al., 2021).

2.8. Toxicity assessment

The toxicity study is the essential step for drug discovery and development. All the phyto-constituent were computationally screened for various type of activity, including mutagenic, tumorigenic, irritant, and reproductive toxicity by OSIRIS data warrior software version 4.5.1 (Gupta et al., 2021).

2.9. Protein preparation

The 3D X-ray protein crystal structure of the main protease (PDB code 6LU7), papain-like protease (PDB code 6W9C), helicase protein (PDB code 5RMD), ACE-2 proteins (PDB code 1O8A, 6LZG and 6M0J) and spike glycoproteins (PDB code 6VYB and 6VXX) were retrieved from the protein data bank server (<https://www.rcsb.org/>). The structure was prepared and purified for molecular docking (Figure 2) (Ahmad, 2019; Contreras-Puentes & Alviz-Amador, 2020; Khan et al., 2018).

2.10. Molecular docking

The active site of protein structure was determined where the active ligand was interacted. This parameter was determined through AutoDock tool. After purification of protein, the three-dimensional map of grid box was made in the receptor site, and docking was performed. The grid box map was determined according to the docking tools. The map was made extensive as a protein active site so that the drug binds itself in all parts of the protein likely to be docked (Tallei et al., 2020).

The AutoDock 4.2 is a free offline docking tool was used to determine the drug-protein interaction. The present study was determined the interaction of the active phytoconstituents of *Moringa oleifera* with different SARS-CoV-2 proteins. Firstly, the protein and ligand BDBQT file was generated. After that, the grid box was generated, and the size of the box was fixed

at 60 Å to all three X, Y and Z coordinate, respectively. The Lamarckian genetic algorithm (LGA) was selected to search for the finest confirmers. The BIOVIA Discovery studios were used to determine the best conformational interaction between the protein and ligands (Ahmad, 2019; Sisakht et al., 2021). Before the initial docking of molecules, the Protein Data Bank's crystal structure of the protein was used to identify the active protein/receptor site. The protein was visualized in discovery studios visualizer then select the existing ligand complex with protein and identify the ligand's attributes, which bound to the specific site of the protein. XYZ coordinates' characteristics were saved than ligand, and the protein PDBQT file and manually the grid box was generated 60 X 60 X 60 around active ligands was identified. The configuration file was generated, and exhaustiveness was set at 8. The molecular docking was performed by using AutoDock vina and determine the highest ligand-protein interaction and correlate with the previous docking study was done by using AutoDock 4.2. they were using Auto dock vina (Contreras-Puentes & Alviz-Amador, 2020; Petit et al., 2021).

2.11. Molecular Dynamic (MD) simulation study

Molecular dynamic simulation is a technique used to understand ligands' molecular structure and the ligand-receptor complex's bio functional relationship (Hospital et al., 2015). In-depth, the molecular dynamic simulation helps to understand the optimal function of proteins in the biological system essential for drug discovery. In the current study, a free online web server called LARMD version 1.0 (<http://chemistry.ang.ccnu.edu.cn/ccb/server/LARMD/>) is available to perform molecular dynamic simulations and analyse drug-receptor interactions using three different modules: standard molecular dynamics (Int mod), normal mod analysis (Nor mod), and steered molecular dynamic simulation (Str mod). The MD simulation result was visualized and analysed on the LARMD web page. The best drug-receptor interaction of *Moringa oleifera* phytoconstituent with SARS-CoV-2 target proteins was selected, uploaded on PDB2PQR server, and electrostatic the receptor under different pH values was prepared. An advanced option was selected for MD simulation time was 3ns (nanoseconds). The submission was returned to the MD simulation result server in components such as PCA, confirmation cluster, dynamic residue cross-correlation, hydrogen bond analysis, and free binding and decomposition energies. The viral protein-ligand interactions were determined by the conventional molecular dynamic simulation (Int_Mod) method (Ang et al., 2020; Dolinsky et al., 2007; Gupta et al., 2021).

3. RESULTS AND DISCUSSION

Medicinal plants are widely used for the treatment of different viral or non-viral infections (Imran et al., 2016). The *Moringa oleifera* is a magical plant that contains various properties, including antiviral activity (Nworu et al., 2013), antibacterial (Amabye & Tadesse, 2016), antioxidant (Das

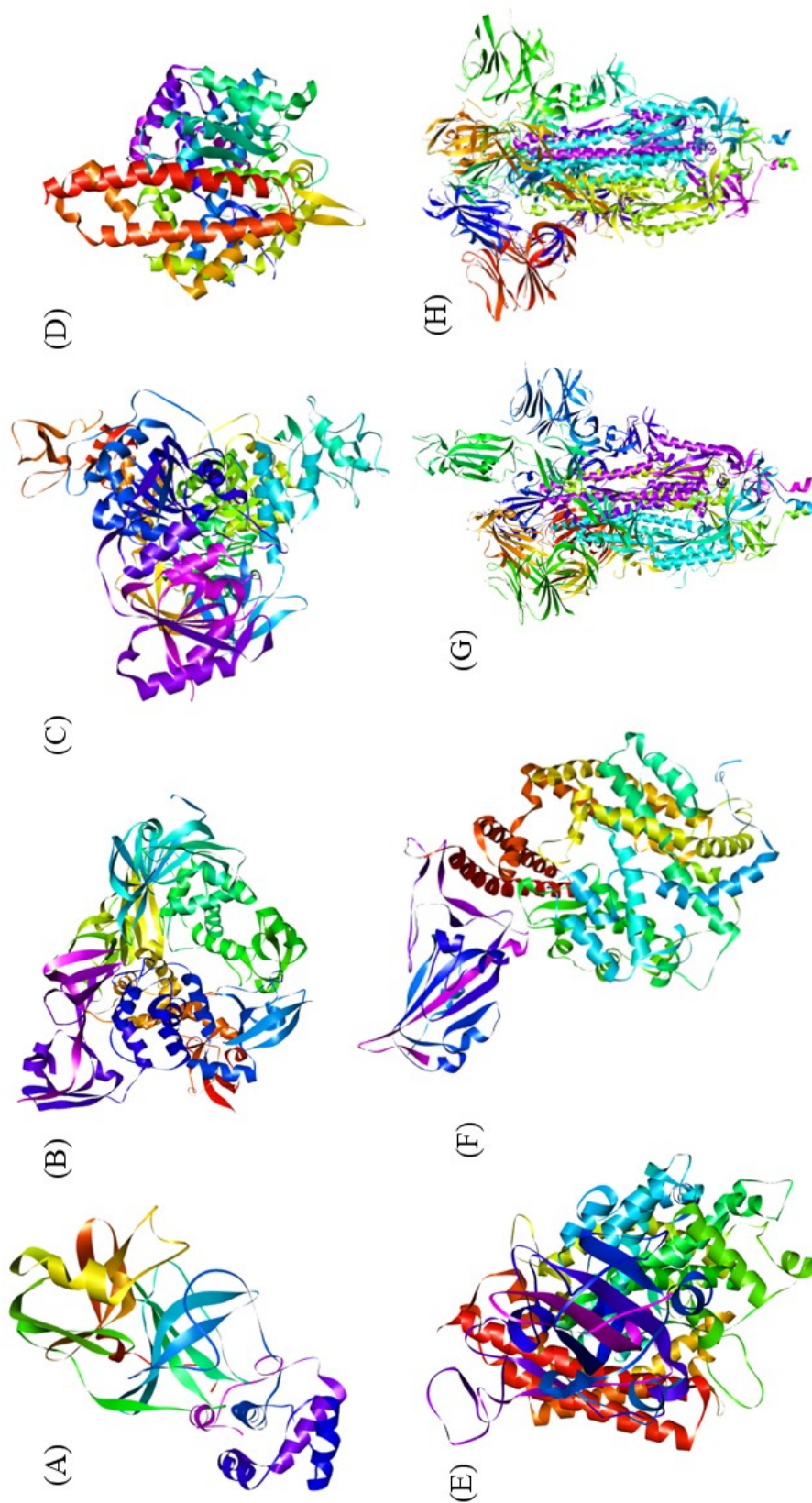


Figure 2. Crystal structure of protein (A) main protease (PDB: 6LU7), (B) Papain-like protease (PDB: 6W9C), (C) Helicase protein (PDB: 5RMD), (D): ACE-2 protein (PDB: 6M0J), (E) ACE-2 protein (PDB: 6LZG), (F) ACE-2 protein (PDB: 6VXX), (G) Spike protein (PDB: 6VYB), (H) Spike protein (PDB: 6VXX).B

Table 1
Binding energy and dissociation constant of *Moringa oleifera* containing active phyto-constituent versus hydroxychloroquine towards selected target proteins (Main protease, Papain like protease and Helicase) of SARS-CoV-2 by using AutoDock 4.2.6.

S.N.	Ligands	Main Protease (6LU7)			Papain Like Protease (6W9C)			Helicase (5RMD)					
		B.E.	Inhibition constant	H atom	Interacting amino acid	B.E.	Inhibition constant	H atom	Interacting amino acid	B.E.	Inhibition Constant	H atom	Interacting amino acid
1	Beta carotene	-5.3	123.96 μ M	-	Ser143, Asn151, Ser113, Phe112, Gln127	-4.82	293.74 μ M	1	Thr119, Leu120, Gln174, Tyr154	-9.53	102.91 mM	-	Pro179, Ser535, Asn557
2	Myricetin	-6.26	25.97 μ M	6	Phe3, Lys5, Gln288, Trp207, Leu282	-1.77	60.61 mM	2	Gln174, Asn156	-7.56	2.87 μ M	3	Pro408, Leu138, Asn124, Asn381, Ala123, Ala135
3	Phytol	-5.72	64.49 μ M	2	Ala7, Gln127, Met6, Glu288	-1.75	52.3 mM	2	Ser170	-5.61	77.63 μ M	1	Lys146, Tyr180, Tyr228
4	Quinic acid	-4.54	472.07 μ M	4	Trp209, Leu282, Arg4, Lys5	-3.11	5.25 mM	5	Asn156, Tyr154, Arg82, Asp76	-4.53	476.67 μ M	3	Tyr421, Arg409, Asn381, Ala135
5	Quercetin	-6.83	9.84 μ M	3	Phe3, Arg4, Lys5	-5.61	77.78 μ M	4	Asp76, Arg82, Gln174, Cys155	-7.42	3.62 μ M	3	Asn124, Ala123, Asn381, Leu138, Pro408, Ala135, Tyr380
6	Squalene	-6.88	9.11 μ M	-	Lys137	-2.21	23.8 mM	-	Tyr154, Arg166	-4.69	366.16 μ M	-	Glu143, Lys146
7	Vitamin E	-8.09	1.18 nM	1	Lys5	-3.65	2.1 mM	1	Asp76, Arg82	-6.4	20.49 μ M	2	Lys148, Asn179, Val181
8	Hydroxy chloroquine	-6.75	11.25 μ M	3	Lys5, Trp207, Leu282	-1.96	36.8 mM	2	Gln174	-5.53	88.59 μ M	2	Asn179, Glu143, Lys146

et al., 2012), and also contains nutritional components including vitamin C, vitamin D, beta carotene, sterols, etc. (Gopalakrishnan et al., 2016). In this pandemic situation, there is no proven drugs are available to treat SARS-CoV-2 infection. Herbal medicine is a good source for potent constituents to maintain immunity and eradicate pathogens from host cells this is the main objective of this study is to determine the affinity of potential active constituent of *Moringa oleifera* on different SARS-CoV-2 viral proteins. All the constituents of *Moringa oleifera* showed good affinity to counter the replication of viral proteins and have good physicochemical and pharmacological property that helps to maintain the bioavailability of drug into the body.

3.1. PASS analysis

The molecular properties of *Moringa oleifera* contain active phytochemicals versus hydroxychloroquine are summarized in Table S1, Appendix A. All the values of clogP, TPSA, MW, % absorption, Lipinski's violations, hydrogen bond acceptor (HBA), hydrogen bond donor (HBD) were determined of above-mentioned drugs (Meanwell, 2016). The hydrophobicity of the compounds was measured by clogP. The low hydrophobicity and high value of clogP showed poor absorption and permeation of the compound (Kaiser & Valdmanis, 1982). The present study revealed that active phytoconstituent of *Moringa oleifera* (myricetin, quinic acid, quercetin) and standard drug hydroxychloroquine shows good clogP value <5, which indicate that good absorption and permeation through the GI tract. The molecular weight of the compounds of *Moringa oleifera* was <500 that may be effective as compared with previous study (Kumar et al., 2017). The results suggested that the active phyto-constituents of *Moringa oleifera* displayed no violations of Lipinski's rule of five. Thus, the compounds showed good physicochemical parameters of ideal drugs.

3.2. Bioactivity (BAS) and Bioavailability (ABS) Score and Prediction of Drug likeness

The different active phyto-constituents of *Moringa oleifera* behaves like a drug because of good drug score values. The Molinspiration version 2016.17 online software was used to determine the bioactivity score of active phytoconstituents and reference drug hydroxychloroquine concerning human receptors, including G-protein Coupled Receptors (GPCR), ion channel, and enzyme-linked receptor (Protease and kinase) (Ahmad, 2019). According to the BAS rule >0.0, the drug is physiologically active, if it is the range -5.0 to 0.0 is moderately active, and <-5.0 the drug candidate is inactive. All the receptor scores of phytoconstituents and standard drug (Hydroxychloroquine) were found to be >-5.0 shows its bioactivity (Ursu et al., 2011). Drug likeness score of phytoconstituents and reference drug was decreased in the following order Hydroxychloroquine > Quercetin > Myricetin > Quinic acid > Beta carotene > Squalene > Phytol > Vitamin E in Table S2, Appendix A.

SwissADME is an online software used to determine the of pharmacokinetic properties and bioavailability scores of active

drugs. This software has five filters that define an active molecule's drug-like properties, including Lipinski (Ursu et al., 2011), Ghose (Ghose et al., 1999), Veber (Veber et al., 2002), Egan (Veber et al., 2002), and Muegge (Muegge et al., 2001). In the present study indicated that phytoconstituent and reference drug (Hydroxychloroquine) obeys all filters have some violations. Still, it does not exceed the number of 3 violations according to the Lipinski rule of five. The pharmacologically active drugs must have >10% of oral bioavailability in rats (Martin, 2005). All the phytoconstituents of *Moringa oleifera* had a 0.55 ABS score similar to Hydroxychloroquine, and only beta carotene has a 0.17 ABS score. It indicates that all the drugs are conventional to administer orally (Table S3, Appendix A).

Determination of protein target of all phytoconstituents of *Moringa oleifera* was assessed by using SwissADME online software. The observed 25 result was mentioned in pie chart Figure S2, Appendix A. The pie chart of supplementary Figure S2 (A) of beta carotene includes 56% nuclear receptor, 24% G-protein coupled receptor, 8% kinase, Figure S2 (B) myricetin 28% kinase, 20% enzyme, 8% protease, oxidoreductase, and G-protein-coupled receptor Figure S2 (C) phytol includes 28% kinase, 20% enzyme and 12% nuclear receptor, Figure S2 (D) quinic acid 32% enzyme, 20% nuclear receptor and 16% G-protein coupled receptor and fatty acid-binding protein, Figure S2 (E) quercetin 28% kinase and 24% enzyme and 16% G-protein coupled receptor, Figure S2 (F) squalene 32% enzyme, 24% G-protein coupled receptor and 12% nuclear receptor, Figure S2 (G) vitamin E 28% kinase, 20% G-protein coupled receptor, 12% oxidoreductase and enzyme, Figure S2 (H) hydroxychloroquine 56% G-protein coupled receptor and 20% enzyme and others are 4%.

3.3. Evaluation of toxicity

In computational method also determines the harmful effect such as toxicity [Adverse Drug Reaction (ADR), Contraindication (CI)] of compound and chemicals. The unsuitable compounds are eliminated from the drug screening process as they show a detrimental effect on biological systems. In the present study, all the active phytoconstituent of *Moringa oleifera* were used for its toxicity study, such as mutagenic, tumorigenic, reproductive, and irritant effects versus hydroxychloroquine used as a reference by using OSIRIS online software. The hydroxychloroquine, quinic acid, and myricetin show potent mutagenic effects, but only quercetin shows mutagenic and tumorigenic effects represented in Table S4, Appendix A. The remaining phytoconstituents were displayed no toxicity effect. However, all those compounds show a toxic effect for structural modification through the structure-activity relationship (SAR) method will be reduces their toxicity.

3.4. Determination of Pharmacokinetic Properties

In Table S5, Appendix A, represents the pharmacokinetic properties of all active phyto-constituent of *Moringa oleifera* using SwissADME online software. This study found that

all active compounds are unlikely to be digested and rapidly absorbed from the GI tract. It was indicated that all the compounds-maintained plasma concentration and increase bioavailability. The reference drug hydroxychloroquine also showed higher absorption and good plasma concentration and bioavailability. All the compounds can cross the Blood-Brain Barrier (BBB) except hydroxychloroquine; thus, it shows the less Central Nervous System (CNS) adverse effect and toxicity to those drugs that have good BBB permeation, thereby it was improved the pharmacological properties of molecules (Aniyery et al., 2015). Similarly, myricetin, quercetin, squalene, and hydroxychloroquine were predicted and there are not to behave like P-gp substrate like hence it was clearly indicated that all these compounds are efflux with the help of glycoproteins and prevent the development of resistance; on the other hand, beta carotene, phytol, quinic acid, and vitamin E are likely to behave as like P-gp substrate thus it increases the sensitivity of glycoprotein and enhance the possibility of drug resistance. All the active compounds of *Moringa oleifera* and reference drug hydroxychloroquine were predicted to behave as CYP1A2 inhibitors; thus, all the compounds except quercetin and hydroxychloroquine were less susceptible to be metabolized and rendered, on the other hand, only quercetin behaves CYP2D6 and CYP3A4 inhibitor, which means it decreases the elimination and metabolism, increasing the bioavailability of the drug.

3.5. High throughput screening analysis using SwissADME

The high throughput screening helps for determining the Drug like molecules through biochemical screening. In Table S6, Appendix A shows the biochemical properties of all active phytoconstituent of *Moringa oleifera* versus the reference drug hydroxychloroquine (Brenk et al., 2008). The molecules to be observed in Pain Assay Interference Compounds (PAINS), Brenk and lead likeness with synthetic associability score (SAS) of beta carotene 6.19, myricetin 3.27, phytol 4.30, quinic acid 3.34, quercetin 5.28, squalene 4.73, Vitamin E 5.17 and reference drug hydroxychloroquine 2.82 thus adequate and suitable compounds myricetin (zero violation), quinic acid (1 violation) and hydroxychloroquine (2 violation) were showed drug like molecules (Ertl & Schuffenhauer, 2009; Hann & Keserü, 2012; Teague et al., 1999).

3.6. BOILED-Egg

BOILED-Egg model was used to determine the gastrointestinal absorption and blood Brain Barrier permeability. The white zone shows the physiochemical space of molecules with the highest GI absorption, and the yellow zone represents the highest possibility of molecules reaching into the brain. This study was accessed through SwissADME online tool. In Table S5 and Figure S5 Appendix A, was described the all the parameters of active constituents of *Moringa oleifera* versus hydroxychloroquine as a reference drug. Previously Gupta A. et al., was determined the physiochemical properties of selected compounds and the result showed that morin expressed in white

region whereas the hydroxychloroquine obeys in yellow (Gupta et al., 2021). The result stat that morin have highest absorption through GI system. Similar result was found in present study. The most of phyto-constituents were obeys in white region as compared with reference drug (hydroxychloroquine).

3.7. Bioavailability radar

The SwissADME online prediction software, the evidence showed that hydroxychloroquine (HCQ) and zone C and E have the optimal range of all the mentioned six properties. The other active compounds of *Moringa oleifera* are failed to obeyed the optimal properties of ideal candidates. Still, they all have obeyed more than one property (Figure S4 and Table S7, Appendix A). Previous study was done by Trivedi A. et al., represented that the selected natural compounds against SARS-CoV-2 protein, was determined the drug like properties by using bioavailability radar. The result showed that most of compounds obeys into the pink zone which was considered as a drug like molecule (Trivedi et al., 2021). In the present study similar result was found of selected phyto-constituents.

3.8. Molecular docking

In present study depicted the molecular docking result of all active phytoconstituent of *Moringa oleifera* versus hydroxychloroquine with the target viral proteins of SARS-CoV-2 was calculated by using AutoDock 4.2.6 software and for docking validation was done by using AutoDock Vina. The result of selected proteins and ligand complexes were visualized by using BIOVIA Discovery Studio 13.0 and 17.1, and 3D representations of the best docking poses of all ligand complexes were included in S8-S15, Appendix A. Similarly, in Table 1 the result of AutoDock 4.2.6 revealed that vitamin E with the main protease of SARS-CoV-2 showed the highest binding affinity, was (-8.09 K_d value 1.18 nM) similarly the beta carotene and myricetin with helicase protein has the highest interaction was (-9.53 K_d value 102.91 nM and -7.56 K_d value 2.87 μ M) respectively. At the same time, the interaction of selected active constituents with ACE-2 receptor proteins showed that beta-carotene has highest interaction and binding energy with all proteins, but with PDB ID 1o8A showed more interaction was -12.05, K_d value 1.46 nM in Table 2. Vitamin E, squalene, and beta carotene with spike glycoproteins of SARS-CoV-2 showed significant interaction compared with reference hydroxychloroquine drug. The result showed that vitamin E with both spike proteins (6VYB and 6VXX) showed the highest interaction (-8.87 K_d value 314.99 nm and -8.34 K_d value 765.09 nM), similarly other drugs including squalene binding energy -8.42 K_d value 677.84 nM and beta carotene binding energy -7.27 K_d value 4.72 μ M also showed good interaction with spike glycoprotein PDB ID 6VYB. Whereas the hydroxychloroquine the binding energy -7.24 K_d value 4.92 μ M and -7.38 K_d value 3.87 μ M represented that the reference drug also had the strongest interaction with both spike glycoprotein (6VYB and 6VXX), but it was observed that the least interaction as compared with vitamin

Table 2
Binding energy and dissociation constant of *Moringa oleifera* containing active phyto-constituent versus hydroxychloroquine towards selected different ACE-2 target proteins of SARS-CoV-2 by using AutoDock 4.2.6

S.N.	Ligands	ACE-2 Protein (PDB ID: 1o8A)			ACE-2 Protein (PDB ID: 6LZG)			ACE-2 Protein (PDB ID: 6MOJ)					
		B.E.	Inhibition constant	H atom	Interacting amino acid	B.E.	Inhibition constant	H atom	Interacting amino acid	B.E.	Inhibition Constant	H atom	Interacting amino acid
1	Beta carotene	-12.05	1.46 nM	-	Tyr394, Glu403, Val380, Glu376, Ala356	-9.77	68.86 nM	-	His401, Tyr515, Arg518	-10.2	33.59 nM	-	Phe390, Arg393, Asn394, Acp382
2	Myricetin	-6.87	9.25 μ M	5	Asn70, Glu384, Tyr523, Glu411	-5.99	40.49 μ M	5	Asp382, His378, Glu402, Glu398, His401, Arg393, Tyr305	-5.73	63.31 μ M	4	Ala348, His378, Glu402, Glu398, His401, Arg393, Asn394
3	Phytol	-5.6	78.77 μ M	1	His410, Glu411, His353, Ala356	-4.98	221.92 μ M	2	Asp392, Tyr385, Leu391	-4.76	322.72 μ M	2	Phe390, Asp382, Glu398, Arg393
4	Quinic acid	-3.82	1.58 mM	5	Ala354, Ala356, Gln411, Tyr523	-3.97	1.22 mM	3	Asn394, Lys552, Leu391, Arg393, Phe390	-3.62	2.21 mM	4	Asn394, Lys562, Leu391, Arg393, Phe390
5	Quercetin	-6.01	39.35 μ M	4	Glu162, Lys511, Gln231, Tyr520, His383, Asp415	-5.84	49.82 μ M	5	Ala348, Asp250, Asn394, Arg393	-6.49	17.44 μ M	5	Ala348, Asp350, Asn394, Arg393, Phe390, Leu351, Gly352
6	Squalene	-6.81	10.23 μ M	-	His383, Glu411	-6.23	26.96 μ M	-	Phe390, Asp350, Arg393	-6.67	12.99 μ M	-	Asp382, Arg393, Glu398, Tyr385
7	Vitamin E	-6.68	12.75 μ M	2	Asp415, Fln281, Glu384	-7.54	2.97 μ M	1	Phe40, Ser44, Asn394, Asp350	-6.71	12.01 μ M	1	Phe390, Trp349, Ala348
8	Hydroxy chloroquine	-5.66	70.9 μ M	4	His383, Asp415, Asp452, Thr282, Glu376, Thr520	-5.99	40.63 μ M	4	Ala348, Asp382, Tyr385, Ser44, Trp349	-6.05	36.9 μ M	3	Trp349, Ala348, Asp382, Tyr385, Ser44

Table 3

Binding energy and dissociation constant of *Moringa oleifera* containing active phyto-constituent versus hydroxychloroquine towards selected different Spike glycoproteins of SARS-CoV-2 by using AutoDock 4.2.6.

S.N.	Ligands	Spike protein (PDB ID: 6VYB)			Spike Protein (PDB ID: 6VXX)		
		B.E.	Inhibition constant	H atom	B.E.	Inhibition constant	H atom
1	Beta carotene	-7.27	4.72 μ M	-	-4.07	1.05 μ M	-
2	Myricetin	-6.87	9.25 μ M	5	-6.23	27.24 μ M	4
3	Phytol	-6.11	33.13 μ M	1	-6.03	37.76 μ M	2
4	Quinic acid	-4.46	537.78 μ M	2	-3.82	1.59 mM	2
5	Quercetin	-7.38	3.92 μ M	4	-5.73	63.46 μ M	2
6	Squalene	-8.42	677.84 nM	-	-4.08	1.3 mM	3
7	Vitamin E	-8.87	314.99 nM	2	-8.34	765.09 nM	1
8	Hydroxychloroquine	-7.24	4.92 μ M	3	-7.38	3.87 μ M	4

Table 4
Binding energy and dissociation constant of *Moringa oleifera* containing active phyto-constituent versus hydroxychloroquine towards selected target proteins (Main protease, Papain like protease and Helicase) of SARS-CoV-2 by using AutoDock vina.

S.N.	Ligands	Main Protease (6LU7)		Papain-Like Protease (6W9C)		Helicase (5RMD)		
		B.E.	Diss. Constant (Kd)	B.E.	Diss. Constant (Kd)	B.E.	Diss. Constant (Kd)	
1	Beta carotene	-9.2	186.45 nM	-7.2	4.58 μ M	-6.8	10.28 μ M	His230, Pro335, Leu352, Ala362, Pro364
2	Myricetin	-7.8	1.89 μ M	-6.9	8.22 μ M	-6.3	24.29 μ M	Met233, Pro234, Ser236, Asn361, Val386, Ala389
3	Phyrol	-4.9	238.59 μ M	-4.4	597.02 μ M	-4.9	238.59 μ M	Pro335, Arg337, Leu363
4	Quinic acid	-5.6	74.91 μ M	-5.0	195.17 μ M	-4.4	597.02 μ M	His230, His311, Ala338
5	Quercetin	-7.8	1.91 μ M	-6.9		-6.0	38.56 μ M	Pro234, Ser236, Leu363, Glu365, Arg390
6	Squalene	-6.8	10.26 μ M	-4.9	238.59 μ M	-4.7	394.17 μ M	Pro234, Ser236, Leu363, Glu365, Val386, Ala389, Arg390
7	Vitamin E	-7.0	7.28 μ M	-5.4	98.89 μ M	-7.9	1.62 μ M	His230, Met233, Pro335, Arg337, Arg390
8	Hydroxychloroquine	-6.6	357.27 μ M	-5.6	72.08 μ M	-5.5	79.36 μ M	His311, Asn31, Tyr382, Val386, Tyr273

E, similarly in comparison with other active phytoconstituents like squalene and beta carotene the hydroxychloroquine had higher interaction with 6VXX spike glycoprotein (Table 3). Previous study done by Belhassan et al. (2022) was reported that β -carotene and tocopherol showed good interaction with SARS-CoV-2 main protease was -6.5 and -6.3 Kcal/mol value respectively. This study revealed that both compounds were capable to inhibit the viral protein synthesis (Belhassan et al., 2022). Whereas in present study showed that tocopherol (vitamin E) has highest interaction was -8.09 K_d value 1.18 nM and beta carotene was showed least interaction -5.3 K_d value 123.96 μ M respectively. Another previous study showed that alpha tocopherol showed satisfying inhibition of main protease was -5.1 Kcal/mol, while glutathione showed highest and similar interaction of reference with same viral protein was -6.0 and -6.2 Kcal/mol respectively (Linani et al., 2022).

The docking validation with AutoDock Vina of same active phytoconstituents and proteins with all active site attributes were used. In Table 4, beta carotene showed the best interaction with the main protease, papain-like protease, and helicase proteins but with the main protease had better interaction was (-9.2 K_d value 186.45 nm), while myricetin and Quercetin showed similar interaction (-7.8 K_d value 1.89 μ M and -7.8 K_d value 1.91 μ M), these three active constituents of *Moringa oleifera* showed the highest interaction as compared with other active phytoconstituent and reference drug hydroxychloroquine respectively.

All the active phytoconstituents of *Moringa oleifera* with ACE-2 proteins showed good interaction with beta carotene, and squalene with PDB ID 1o8A showed the highest interaction with the binding energy dissociation constant was -10.7 K_d value 9.91 nM and -9.9 K_d value 214.28 similarly, other phytoconstituents also showed strong interaction. The other ACE-2 proteins 6LZG and 6MOJ, interact with these phytoconstituents. The result revealed that the binding energy of all phytoconstituents was closer to each other. In the present study observed that beta carotene, myricetin, and quinic acid had good interaction, whereas hydroxychloroquine had the highest interaction with all three ACE-2 proteins. The HCQ with 1o8A binding energy -9.1 K_d value 214.28 nM was determined, but it was observed that least interaction with beta carotene similarly, with 6MOJ protein, the binding energy of beta carotene and HCQ is same, which was -9.0 Kcal/mol (Table 5).

In SARS-CoV-2 spike glycoproteins, PDB ID 6VYB and 6VXX interact with all active phytoconstituents of *Moringa oleifera* showed stronger binding affinity. The beta carotene with both proteins had the strongest action compared to other phytoconstituents -9.1 K_d value 190.32 nM and -8.5 K_d value 534.67 nM; similarly other constituents showed similar binding energy. The hydroxychloroquine also had a similar binding affinity -8.6 K_d value 443.93 nM and -8.4 K_d value 718.47 nM was found to be least interaction compared to beta carotene (Table 6).

The present study determines the interaction of other SARS-CoV-2 viral proteins responsible for replicating the viral genome into the host cell. The active phytoconstituents of *Moringa oleifera* showed the highest interaction with ACE-2 receptor and spike glycoproteins of the SARS-CoV-2 virus.

3.9. Molecular Dynamic (MD) Simulation

The study of the thermodynamics of biological molecules and their complexes, as well as structural confirmation and variation over time, is significantly assisted by molecular dynamic (MD) simulation. In Figure 3 - Figure 11 represent the MD simulation of different active phytoconstituents including beta carotene, vitamin E, and myricetin with SARS-CoV-2 viral proteins such as PDBID-1o8A, 6LZG, 6MOJ, PDBID 6VYB and 6VXX of by using Int_mod. For 3ns, RMSD, RMSE, radius of gyration (rg), and function of native contacts analyses were used to determine the stability of the ligand and protein complex. The Root Mean Square Deviation (RMSD) value helps to analyse the average distance between the atoms of overlapped structure. The MD simulation analysis showed an adequate stability profile of different protein-ligand complexes at 300 k temperature. The beta carotene and ACE-2 receptor 6MOJ complex revealed very low but constant deviation in the RMSD graph from 1.0 to 2.5 Å throughout the 3 ns MD simulation analysis (Figure 3b). Similarly, myricetin and 6MOJ complex displayed less deviation in RMSD from 0.5 to 1.5 Å at the same time scale (Figure 9b). The vitamin E and spike glycoproteins PDB ID 6LZG complex at same time scale 3 ns of MD simulation analysis showed that for 0.25 to 1.0 Å RMSD valued was very low at 1500 ps after that it showed 1.5 Å constant deviation 3000 ps time scale (Figure 6b). The RMSD analysis of all complexes suggested that the high stability and compactness of ligand and protein complexes were indicated by the minimal deviation of RMSD value.

The radius of gyration (rg) measured radical distance of a point of axis rotation. The result showed important information on the structural activity and behaviour of proteins. The radius of gyration of beta carotene-6MOJ (Figure 3e), myricetin-6MOJ (Figure 9e) and vitamin E-6LZG (Figure 6e) complexes were found to be around 31.2, 31.0, and 31.2 respectively at a 3 ns time scale. The result revealed that minor changes in the compactness of the complex structure during the MD simulation analysis suggested the strong structural stability of all three ligand-protein complexes. Additionally, the value was calculated and the average fluctuation of all complexes (residue) was observed during simulation analysis. The RMSFs of all three complexes, beta carotene-6MOJ, myricetin-6MOJ, and vitamin E-6LZG were plotted. The RMSF is used to conclude each amino acid's atomic positional fluctuation through CA ($C\alpha$) atom-based calculation. The comparative study of RMSF trajectory revealed that all the amino acids residue in the complex model of beta carotene-6MOJ have fluctuated between 0 to 30 Å (Figure 3g). In contrast, the myricetin-6MOJ complex the RMSF value was fluctuated between 0 to 8 Å (Figure 9g) similarly with vitamin E-6LZG

Table 5
Binding energy and dissociation constant of *Moringa oleifera* containing active phyto-constituent versus hydroxychloroquine towards selected different ACE-2 target proteins of SARS-CoV-2 by using AutoDock vina.

S.N.	Ligands	1o8A			6LZG			6MOJ		
		B.E.	Diss. Constant (Kd)	Interacting amino acid	B.E.	Diss. Constant (Kd)	Interacting amino acid	B.E.	Diss. Constant (Kd)	Interacting amino acid
1	Beta carotene	-	9.91 nM	Val380, Leu375, Glu876	-	773.46 nM	Ser77, Ser106, Lys74, Ser70, Trp69	-	220.67 nM	Leu95, Ala99, Val209, Asp206, Glu208
2	Myricetin	10.7	125.26 nM	Val379, Val380, Glu384	8.1	440.32 nM	Asp206, Glu208, Gly205, Tyr196, Gln102, Pro565, Lys562, Gly564	9.0	395.27 nM	Asn210, Gly205, Lys562
3	Phytol	9.3	1.89 μ M	Leu81, Asn66, Asn65, Ser355	8.7	5.51 μ M	Gly205, Glu208, Val209, Ser511	8.8	3.96 μ M	Phe50, Leu143, Asn149
4	Quinic acid	7.9	72.08 μ M	Ser355, His353	6.9	24.07 μ M	Gln493, His34, Asn33, Arg403	7.0	28.75 μ M	Ser563, Lys562, Trp566, Glu208
5	Quercetin	6.5	443.93 nM	Asp415, Lys454, His383, Glu384	6.2	439.65 nM	Gly205, Glu208, Tyr196	6.0	395.27 nM	Glu288, Val209, Lys562, Asn210
6	Squalene	8.9	101.78 nM	Asn66, Ser355, Arg522, Leu140	8.5	9.13 μ M	Asp350, Phe390	8.8	1.62 μ M	Ser43, Ser44, Arg393
7	Vitamin E	9.9	2.24 μ M	Glu284, Asp415	6.8	5.51 μ M	Phe95, Ser47, Thr347, Ala340	7.0	4.21 μ M	Phe390, Arg393, Phe40
8	Hydroxy-chloroquine	7.7	214.28 nM	Asp415, Val380, Lys54, Asn1281	6.9	930.21 nM	Tyr196, Gln98, Gln102, Gly205	7.3	220.67 nM	Ala99, Leu95, Pro565, Glu56, Trp566
		9.1			8.3			9.0		

Table 6
Binding energy and dissociation constant of *Moringa oleifera* containing active phyto-constituent versus hydroxychloroquine towards selected different spike glycoproteins of SARS-CoV-2 by using AutoDock vina.

S.N.	Ligands	6VYB			6VXX		
		B.E.	Diss. Constant (Kd)	Interacting amino acid	B.E.	Diss. Constant (Kd)	Interacting amino acid
1	Beta carotene	-9.1	190.32 nM	Ala771, Arg765	-8.5	534.67 nM	Arg1019, Ala766, Gly769, Thr768, Arg765, Arg1014, Gln954
2	Myricetin	-8.3	709.93 nM	Ala766, Gln762, Ile1013, Gln1010	-8.8	395.27 nM	Ala958, Arg101, Thr961, Gln773, Glu69, Ile770
3	Phytol	-6.9	7.88 μ M	Gln957, Ala766, Arg765	-7.6	2.39 μ M	Leu962, Gln95, Arg1014, Arg1019, Ala1016
4	Quinic acid	-6.8	9.59 μ M	Gln1005, Gln1002	-6.8	10.28 μ M	Leu66, Arg1000, met740, Ile742
5	Quercetin	-8.4	600.41 nM	Ala766, Gln762, Gln954, Gln1010	-8.4	718.47 nM	Thr961, Ala958, Gln957, Gln762, Gly769, Glu773
6	Squalene	-6.8	10.18 μ M	Glu773, Leu1012, Ala766, Ala958, Arg1014, Arg1019	-8.2	654.97 nM	Thr768, Arg765, Asn764
7	Vitamin E	-7.0	4.21 μ M	Arg765, Asn764	-6.6	16.27 μ M	Asp994, Arg995
8	Hydroxychloroquine	-8.6	443.93 nM	Ala766, Gln762, Gln1010	-8.4	718.47 nM	Gln762, Ala766, Glu769, Glu773, Ala958

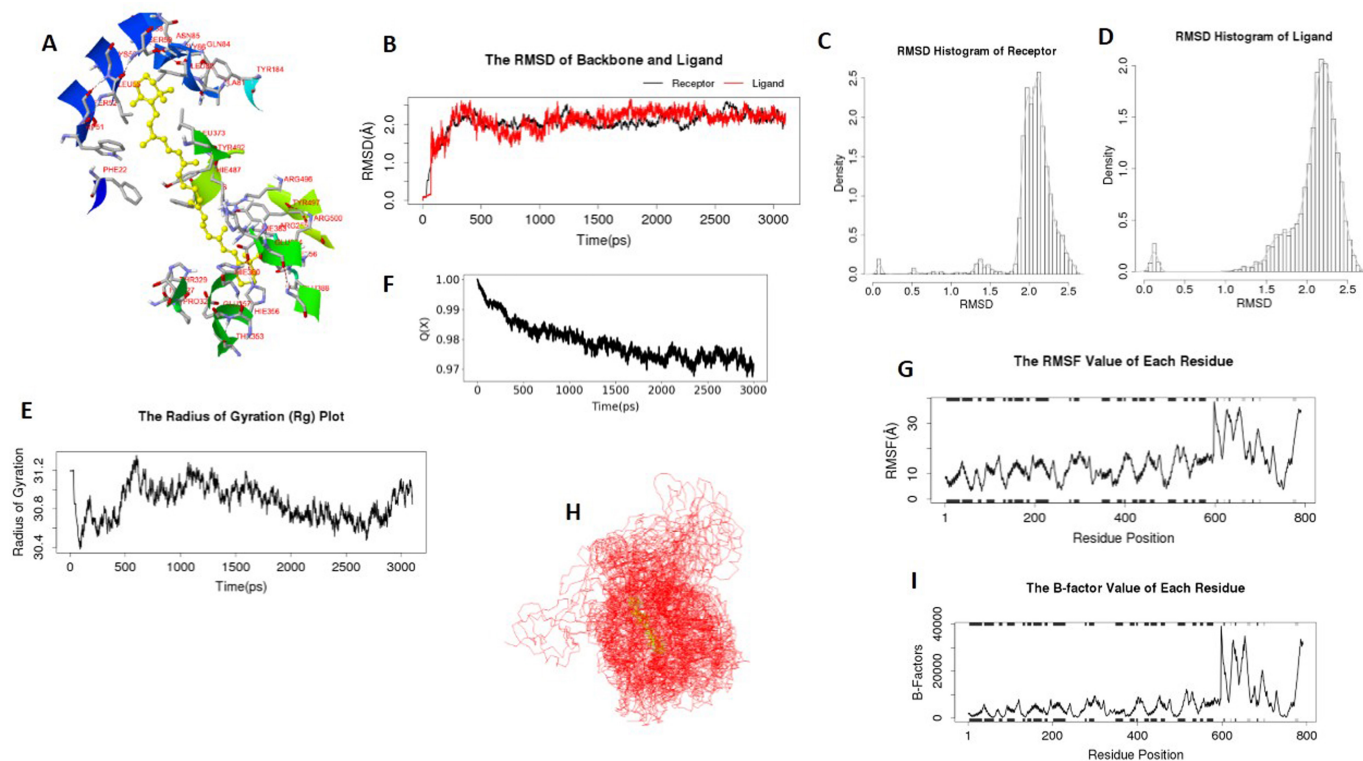


Figure 3. MD Simulation of beta carotene complexed with Angiotensin converting enzyme 2 protein (PDB ID: 6MOJ). (A) Ligand-protein conformation (B) RMSD of receptor and ligand (beta carotene) (C) RMSD histogram of the receptor (D) RMSD histogram of ligand (beta carotene) (E) Radius of gyration, Rg value (F) Fraction of native contacts analysis of ACE-2 with beta carotene over a time frame of 3000ps (3 ns) (G) RMSF value of each residue (H) B-factor value (changing from blue to red with an increase in value) and (I) B-factor analysis of defined complex (Int_mod).

complex the RMSF value has also fluctuated between 0 to 8 Å (Figure 6g) respectively. In the folding method, a definite condition of non-native interaction is considered irrelevant in certain simulation analyses. The folding model only supports the native interactions in energetically favourable conditions. The fraction of native contacts was denoted by $Q(x)$, which helps calculate all proteins transition states beside the free folding energy barrier. The Q_x value of the present study was determined that all three complexes revealed that the relative flexibility and stability was increased during the simulation period, which was 99 % (Figure 3f, Figure 6f, and Figure 9f). In the MD simulation, the B-factor known as temperature factor showed a similar factor of RMSF, which helps explain the attenuation of x-Ray scattering resulting in thermal motion. The B-factor cause the fluctuation of all three complexes around 2000-4000 showed the good stability of complexes Figure 3h,i, Figure 6h,i and Figure 9h,i respectively. The behaviour of conformational differences was perceived by PCA analysis. The extent of pairwise cross-correlation coefficients suggests the atomic system differences related to each other. The correlated residues are shown in blue and uncorrelated residues in red in Figure 4 and 7 and Figure 10. The light pink and blue lines, respectively, represent the paired residues that had greater correlation coefficients (>0.8) and higher non-correlation coefficients (-0.4). The diagram shows black helices,

grey strands, and white loops for secondary structures that are located on the top and right edges of the dynamical residues in cross-correlation map. The MD simulation result was analysed by MM/PB (GB) SA mainly includes various parameters such as electrostatic energy (ELE), van der Waals contributions (VDW), total gas-phase energy (GAS), non-polar and polar contributions of solvations (PBSOL/GBSOL). In the present study, the free binding energy $\Delta PB/\Delta GB$ was recorded, and $PBTOT/GBTOT$ calculated the result, and entropy (TS) was represented in Figure 5a, Figure 8a, and Figure 11a. Similarly, hydrogen bonds were analysed by using various parameters including hydrogen bond acceptor, hydrogen bond donor atoms, average distance of atoms, average angle of atoms, and hydrogen atom proportions (Frac) as represented in Figure 9b,c, Figure 8b,c and Figure 11b,c. Likewise, the result of decomposed electrostatic energy was calculated MM force field (TELE), van der Waals contributions MM (TVDW), a sum of non-polar and polar contributions of solvations (TGBSOL), total gas-phase energy (TGAS), and estimation of binding free energy from TGBTOT, depending on free binding energy the residue and with their contribution rank of top 10 decompose calculation was arranged top to bottom in the heatmap (Figure 5d, Figure 8d, and Figure 11d).

The viral protein crystal structure was retrieved from the protein data bank. Autodock 4.2.6 and Autodock Vina was used

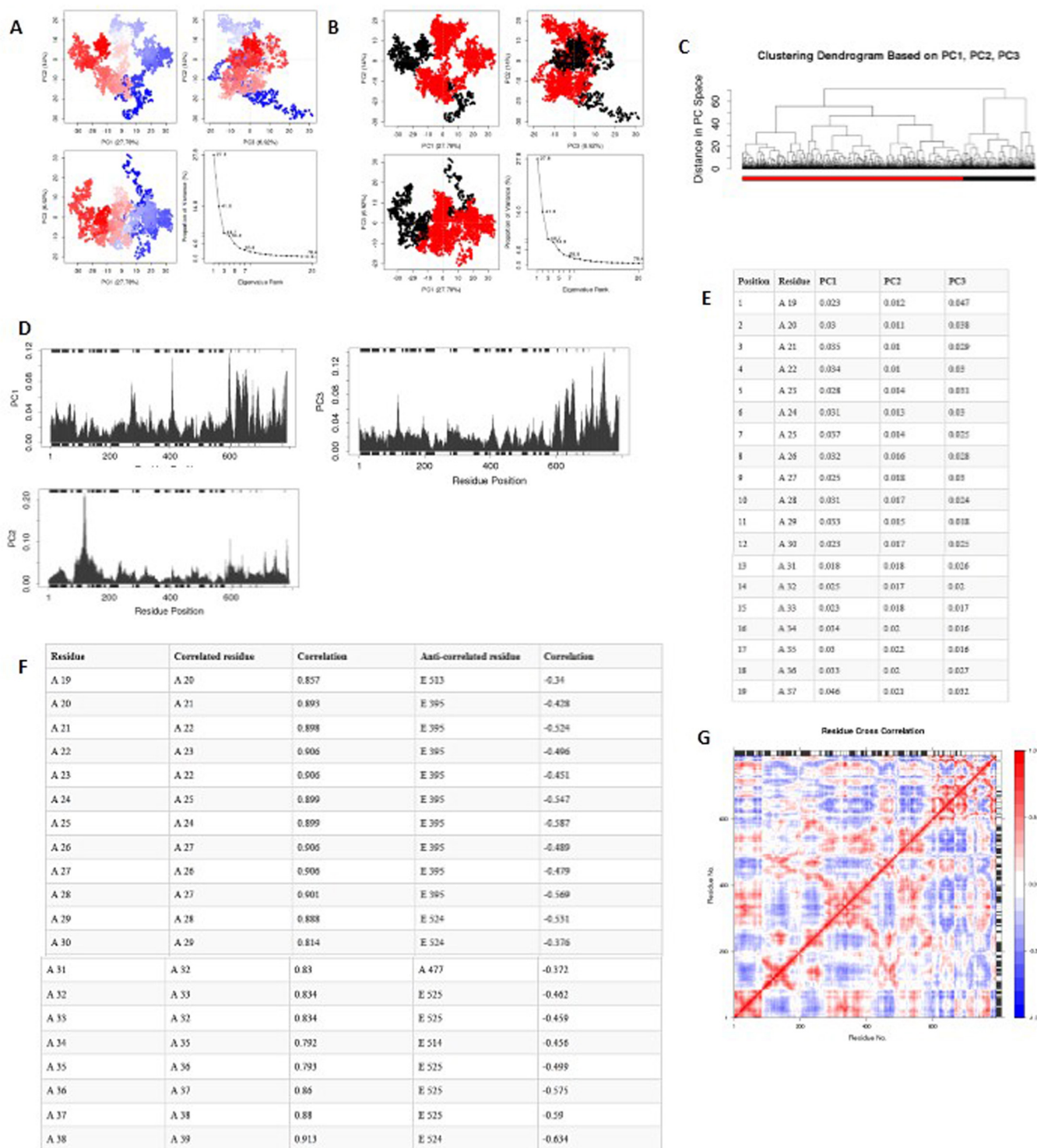


Figure 4. PCA of ACE-2 (PDB ID: 6MOJ) complexed with beta carotene (A) PCA results for Trajectory (B) Simple clustering in PC subspace (C) Clustering dendrogram based on PC1, PC2, and PC3 (D) Residue-wise loadings for PC1, PC2 and PC3 (E) Table data showing residue-wise loadings for PC1, PC2 and PC3 and residue number at each position (F) Table showing pair-wise cross-correlation coefficients; higher correlated coefficient value is >0.8, and higher anti-correlated coefficient value is < 0.4 (G) Dynamical Residue Cross-correlation Map; the correlated residues are in blue, anti-correlated residues are in red; the pairwise residues with a higher correlated coefficient (>0.8) and with a higher anti-correlated coefficient (< 0.4) are linked with light pink and light blue (Int_mod).

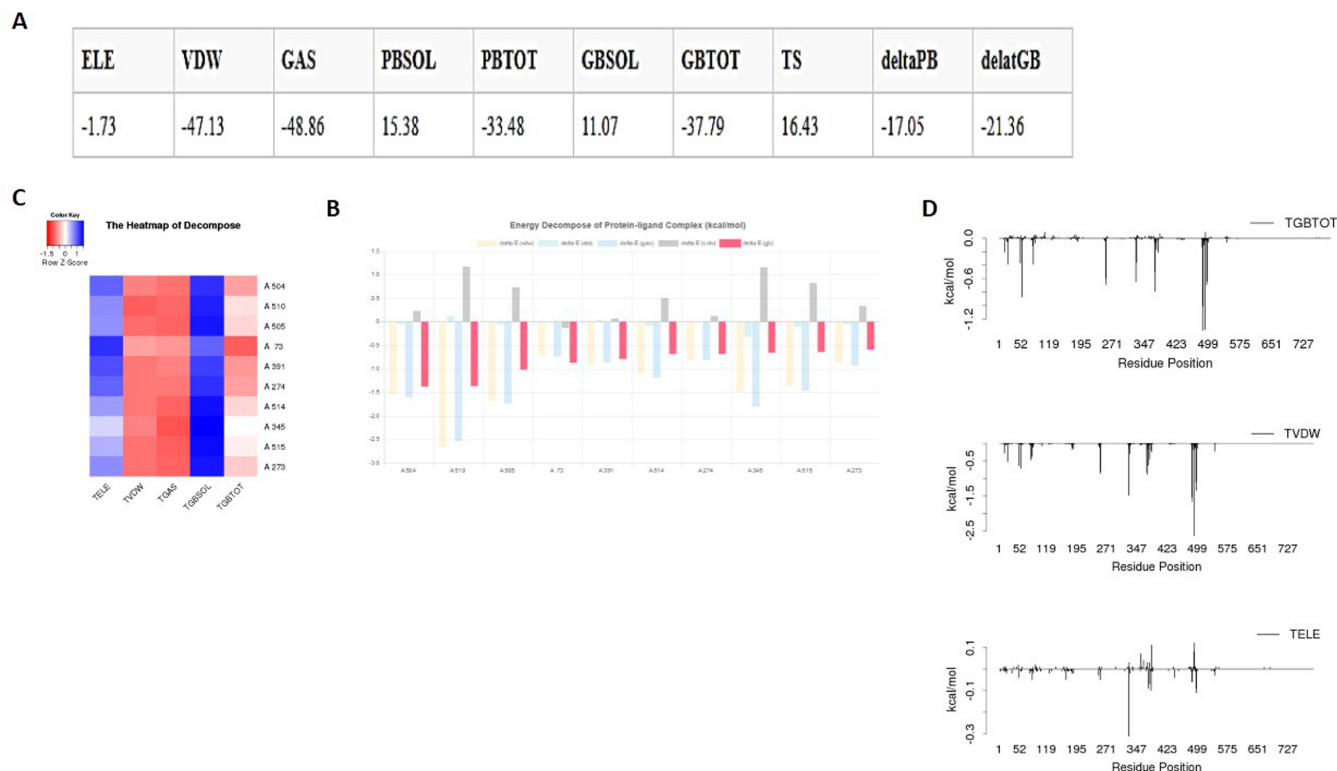


Figure 5. Energy, hydrogen bond analysis and decomposition analysis of ACE-2 protein (PDB ID: 6MOJ) complexed with beta carotene (A)MM/PB(GB)SA result consists of electrostatic energy (ELE), van der Waals contribution (vdW), total gas-phase energy (GAS), non-polar and polar contributions to solvation (PBSOL/GBSOL) (B,C) Statistics of hydrogen bonds (D)Energy decompose of protein-ligand complex (kcal/mol) (E) Graphical representation of decomposing result (F) Heat map of decomposing.

for the analysis of all active constituents of *Moringa oleifera* shows an excellent binding affinity towards selected SARS-CoV-2 viral proteins such as main protease (M-Pro), papain-like protease (PL-Pro), helicase (NSP13), ACE-2 (1o8A, 6LZG, and 6MOJ) and spike glycoproteins (6VYB and 6VXX). After molecular docking, the results were indicated that beta carotene, quercetin, myricetin, and vitamin E showed good interaction with all viral proteins. The binding affinity of the compound with M^{Pro}, PL^{Pro}, and Nsp13 versus reference drug hydroxychloroquine as an order: beta carotene > myricetin > quercetin > vitamin E > hydroxychloroquine > quinic acid.

Coronavirus (CoV) infections commonly affect the respiratory system, digestive system, liver, and central nervous system of humans and animals. This work mainly focused on some important proteins of the SARS-CoV-2 virus is the main protease (3CL^{Pro}/M^{Pro}) PDBID 6LU7, papain-like protease (PL-Pro) PDB ID 6W9C, helicase (Nsp13) PDB ID 5RMD ACE-2 (1o8A, 6LZG and 6MOJ) and spike glycoproteins (6VYB and 6VXX) as a potential target protein of *Moringa oleifera* constituents for COVID-19 treatment. In present study was to identify the new molecules which were inhibited SARS-CoV-2 viral protein replication into the host cells. The drug candidates of *Moringa oleifera* were evaluated on the Lipinski rule. The drug was designed and developed using a cheminformatics tool based on the screening of phytochemical

lead structure. The Lipinski rule of five was determined by using OSIRIS software. Similarly, physicochemical parameters included molecular weight, topological polar surface area, clog P, hydrogen bond acceptor, hydrogen bond donor pharmacokinetics, and pharmacodynamics (receptor-interacting affinity and toxicity study), were calculated before performing the docking. Only those candidates were selected in the present study, which did not have more than 2 violations. The Lipinski rule of five is accepted to all compounds in this study and shows ideal candidates for docking represented in Tables 1, 2 and 4 and Table 5. The drug-likeness and biochemical properties are important parameters for the identification of ideal drug candidates. It defines whether the molecules behave like drugs or not; therefore, Table 3 and Table 6 calculated properties for ideal drug candidates using SwissADME software. Previous study represented the Brain and Gastrointestinal Estimated Permeation Analysis (BOILED-Egg) properties. The result showed that the test molecules of Morin and baricitinib are ideal candidates. They have a higher possibility of absorbing from the GI tract, similar in the present study; the selected active phytoconstituent only quercetin shows the higher possibility of absorbing from GI system (Figure S2, Appendix A) (Gupta et al., 2021). In figure S3 and table S7, Appendix A represents the test compounds phytol and reference drug hydroxychloroquine both fall in the

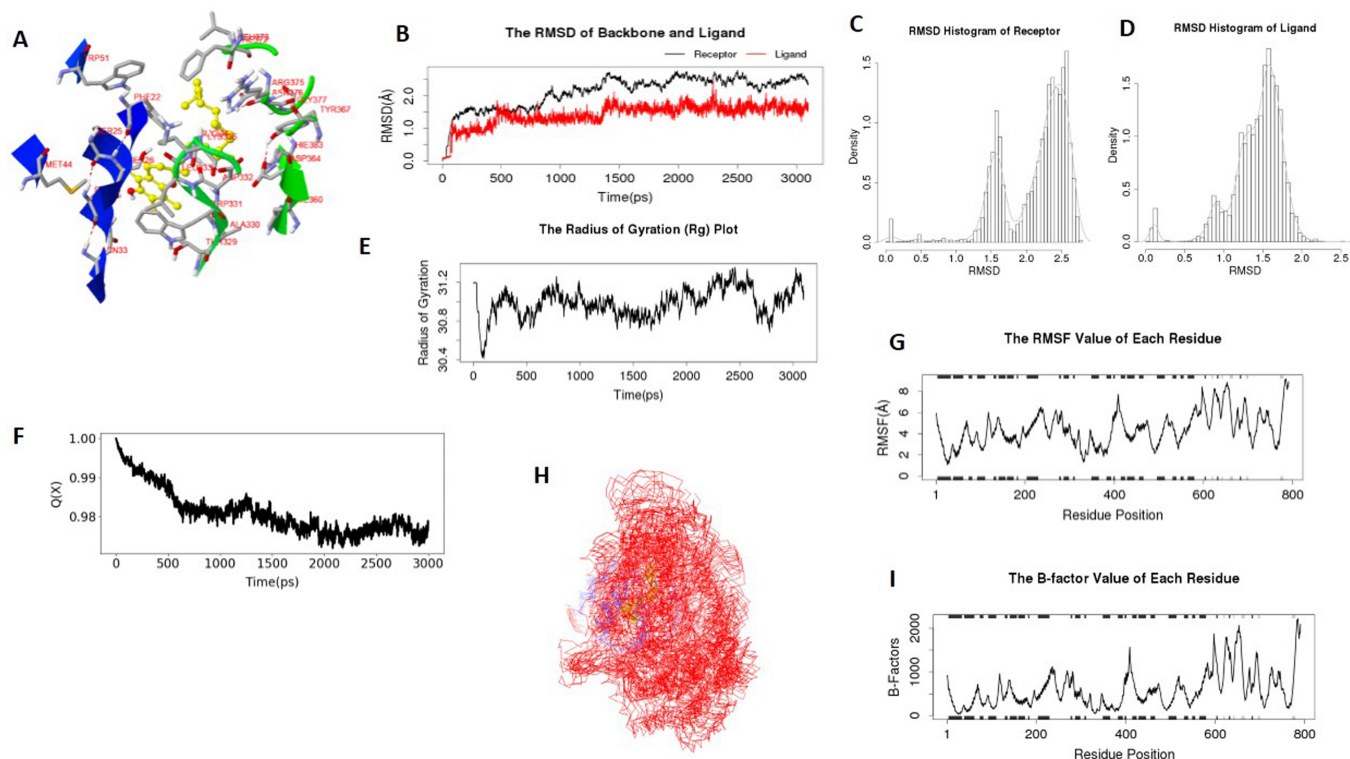


Figure 6. MD Simulation of vitamin E complexed with Angiotensin converting enzyme 2 protein (PDB ID: 6MOJ). (A) Ligand-protein conformation (B) RMSD of receptor and ligand (vitamin E) (C) RMSD histogram of the receptor (D) RMSD histogram of ligand (vitamin E) (E) Radius of gyration, Rg value (F) Fraction of native contacts analysis of ACE-2 with vitamin E over a time frame of 3000ps (3 ns) (G) RMSF value of each residue (H) B-factor value (changing from blue to red with an increase in value) and (I) B-factor analysis of defined complex (Int_mod).

optimal range; therefore, they have good oral bioavailability similarly other molecules also obeyed more than one property as compared to the previous study these compounds have better pharmacokinetic properties, and they follow all parameters for ideal drug candidates. Better bioavailability shows better pharmacological action (Gupta et al., 2021; Kadri & Aouadi, 2020). The seven active phytoconstituent including beta carotene, myricetin, phytol, quinic acid, quercetin, squalene, and vitamin E) of *Moringa oleifera* versus hydroxychloroquine used as a reference compound were docked by using Autodock 4.2.6, and the docking result was validated by using AutoDock vina software. The results showed a significant binding affinity of ligands with all target viral proteins. After that the docking analysis, the drug ligand complex was visualized by using BIOVIA discovery studios 13.0 and 17.1. The active phytoconstituents of *Moringa oleifera* with main protease, papain-like protease, and helicase showed good binding affinity was displayed in Table 1. The vitamin E with main protease had higher interaction BE -8.09 kd 1.18 nM similarly the other active constituents like beta carotene, and quercetin showed significant binding affinity with papain like protease (BE -4.83 kd 293.74 μ M and -5.61 kd 77.78 μ M) and with helicase (BE -9.53 kd 102.91 nM and -7.42 kd 3.62 μ M) the myricetin had also similar binding affinity of quercetin which was (BE -7.56 kd 2.78) versus reference drug hydroxychloroquine (-1.96 kd

36.8 mM and -4.59 kd 88.59 μ M).

The ACE-2 protein is very important for the SARS-CoV-2 virus. With the help of this protein, the viral genome is easily entered into the host cell. It down regulates the immunological response, contributing to multiple organ dysfunction, especially lungs and heart (Ni et al., 2020). In Table 2, different structural proteins of ACE-2 were docked with active constituents of *Moringa oleifera* was to determine the good binding affinity. The beta carotene showed the strongest interaction with 1o8A (BE-12.05 kd 1.46 nM), 6LZG (-9.77 kd 68.86 nM), and with 6MOJ (BE -10.2 kd 33.59 nM) as compared to other phytoconstituents of *M. oleifera* and reference drug hydroxychloroquine. A previous study was done by Gupta et al. (2021) was selected the same protein and docked it with morin. The result revealed that morin had a higher binding affinity and compact interaction with these three proteins (Gupta et al., 2021).

The spike glycoproteins are generally found over the surface of SARS-CoV-2. It appears like a crown. These spike proteins' role provides a support during with the attachment of SARS-CoV-2 with host ACE-2 receptor. After the attachments, the spike proteins are phosphorylated and related to the genomic sequence into the cell for its replication (Ang et al., 2020;?,?). A previous study was done by Trivedi et al. (2021) with spike glycoprotein 6VXX and epigallocatechin, piperine, and

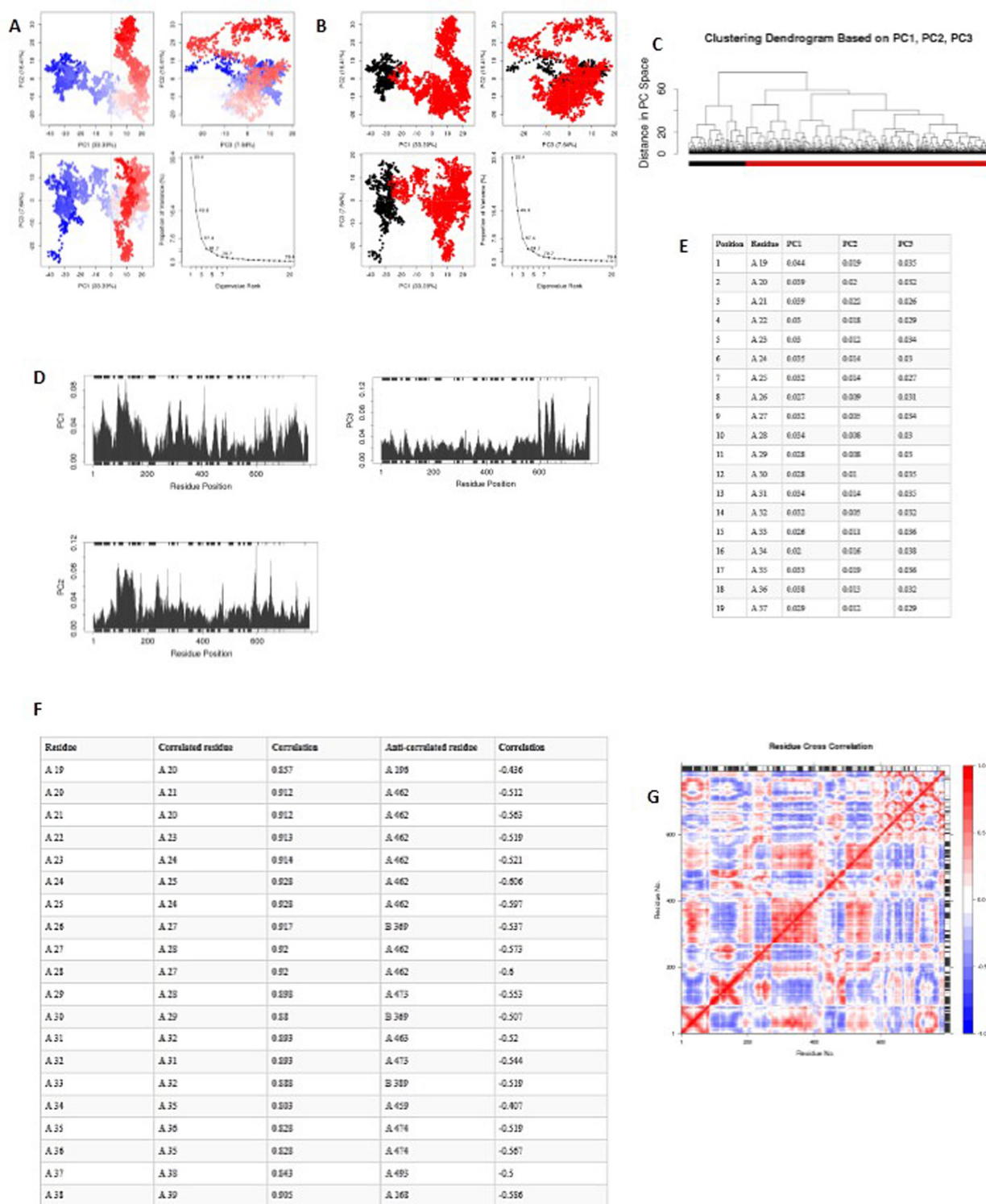


Figure 7. PCA of ACE-2 (PDB ID: 6MOJ) complexed with vitamin E (A) PCA results for Trajectory (B) Simple clustering in PC subspace (C) Clustering dendrogram based on PC1, PC2, and PC3 (D) Residue-wise loadings for PC1, PC2 and PC3 (E) Table data showing residue-wise loadings for PC1, PC2 and PC3 and residue number at each position (F) Table showing pair-wise cross-correlation coefficients; higher correlated coefficient value is >0.8, and higher anti-correlated coefficient value is < 0.4 (G) Dynamical Residue Cross-correlation Map; the correlated residues are in blue, anti-correlated residues are in red; the pairwise residues with a higher correlated coefficient (>0.8) and with a higher anti-correlated coefficient (< 0.4) are linked with light pink and light blue (Int_mod).

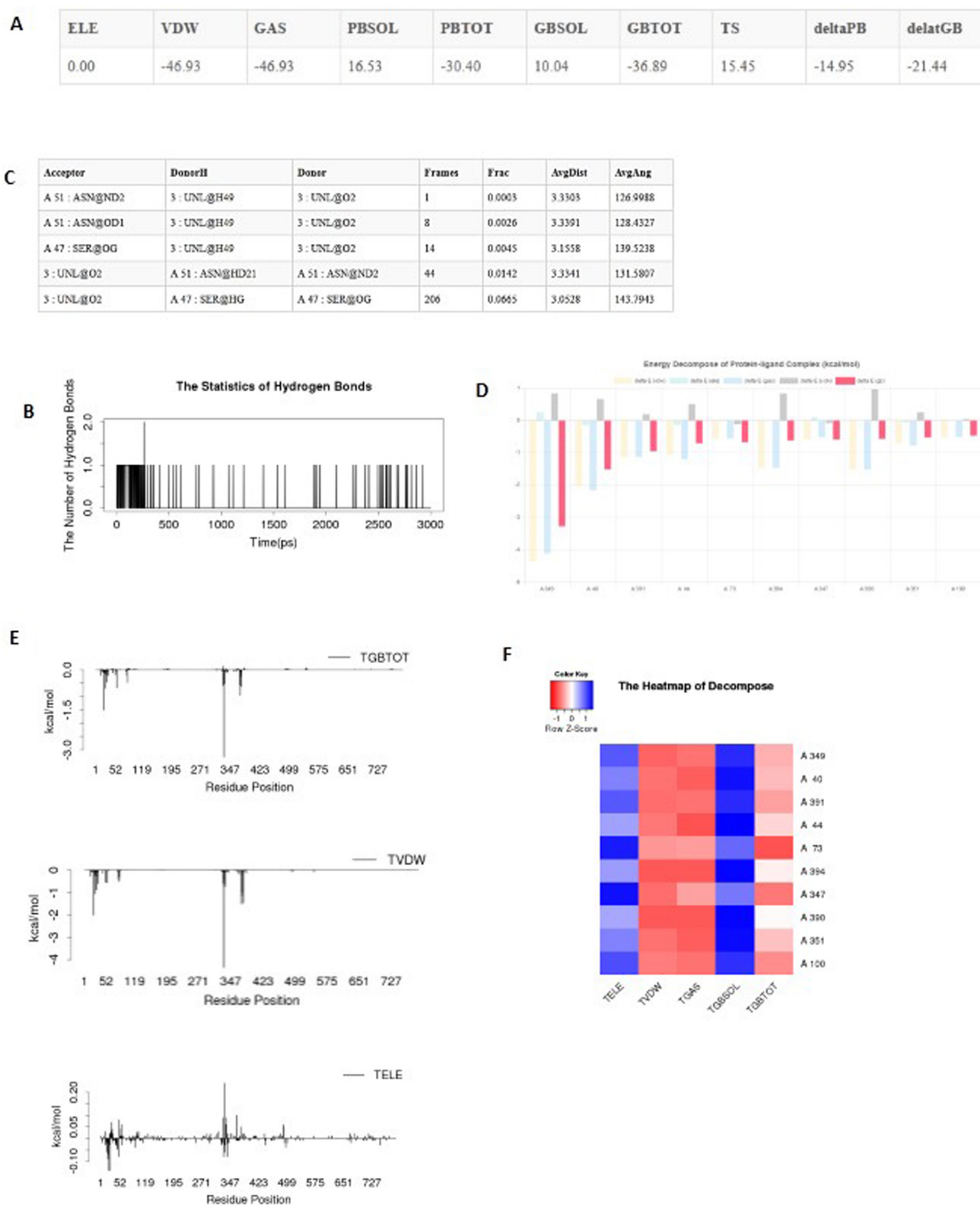


Figure 8. Energy, hydrogen bond analysis, and decomposition analysis of ACE-2 protein (PDB ID:6MOJ) complexed with vitamin E (A) MM/PB (GB) SA result consists of electrostatic energy (ELE), van der Waals contribution (vdW), total gas-phase energy (GAS), non-polar and polar contributions to solvation (PBSOL/GBSOL) (B, C) Statistics of hydrogen bonds (D) Energy decompose of protein-ligand complex (kcal/mol) (E) Graphical representation of decompose result (F) Heat map of decompose.

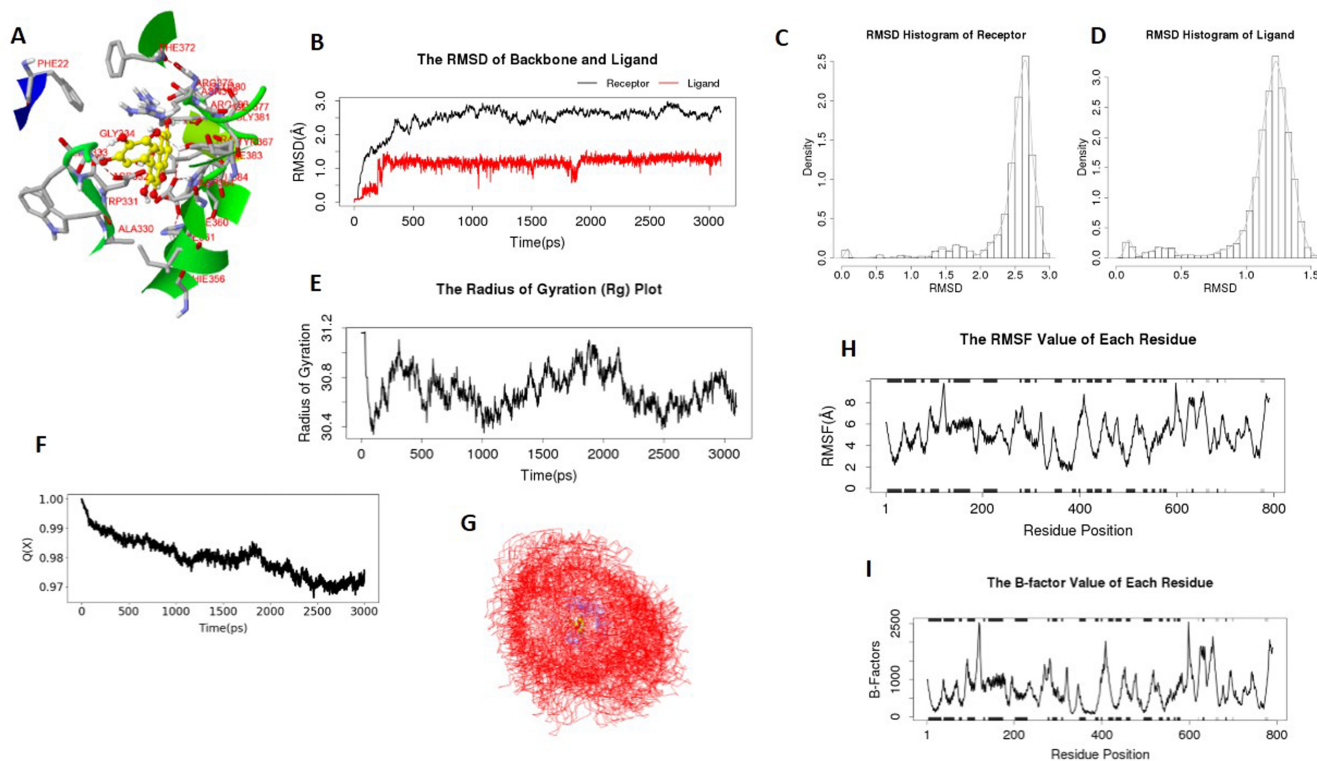


Figure 9. MD Simulation of myricetin complexed with Angiotensin converting enzyme 2 protein(PDB ID: 6MOJ). (A) Ligand-protein conformation (B) RMSD of receptor and ligand (myricetin) (C) RMSD histogram of the receptor (D) RMSD histogram of ligand (Myricetin) (E) Radius of gyration, Rg value (F) Fraction of native contacts analysis of ACE-2 with myricetin over a time frame of 3000ps (3 ns) (G) RMSF value of each residue (H) B-factor value(changing from blue to red with an increase in value) and (I) B-factor analysis of defined complex (Int_mod).

tinosporiasis showed higher binding affinity, which was (BE -8.24 kd 909.72 nM, -7.17 kd 5.59 μ M and -5.07 kd 193.18 μ M) similarly in the present study the vitamin E with spike glycoprotein 6VXX showed maximum binding affinity and strong interaction (BE- -8.34 kd 765.09 nM) while the hydroxychloroquine used as a reference compound showed the least binding affinity which was -7.38 kd 3.87 μ M respectively (Table 3).

In the present study, the docked result from AutoDock 4.2.6 and it was validated by using AutoDock Vina. The result supported that all the active phytoconstituents showed a higher binding affinity with different proteins through AutoDock 4.2.6; similarly, the same phytoconstituents had similar binding affinity was analysed by using AutoDock Vina the result was expressed in Tables 5 and 6 and Table S8, Appendix A. Previous studies also support the result obtained from AutoDock vina with spike glycoprotein 6VXX and all three ACE-2 proteins (Gupta et al., 2021; Trivedi et al., 2021).

The previous study determined the different active phytoconstituents of *Moringa oleifera* by using Gas Chromatography and Mass Spectroscopy (GC/MS) and identifying its antioxidant properties. Additionally, few compounds had the highest concentration percentage in the extract. Strong antioxidant properties were screened, and different phytoconstituents of *Moringa oleifera* were selected for *in-silico* study against the

main protease protein of SARS-CoV-2. The result revealed that apigenin-7-O-rutinoside and mudanpioside showed significant interactions against M-pro protein; similarly, the tipranavir used as a reference drug showed higher binding affinity as comparable with the above phytoconstituents (Nair & James, 2020).

Beta carotene, vitamin E, and myricetin with ACE-2 protein showed strong interaction were subjected to perform MD simulation by using LARMD online server version 1.0. in present study compared with previous studies was done by Gupta et al. (2021); Siddiqui et al. (2022), and Srivastava et al. (2022) showed that similar RMSD deviation of the complexed structure indicated that the active constituents of *Moringa oleifera* such as beta carotene, vitamin E, and myricetin had greater stability with ACE-2 protein throughout 3 ns time scale of MD simulation analysis (Figure 3, 4, 5, 6, 7, 8, 9, 10 and 11) (Gupta et al., 2021; Siddiqui et al., 2022; Srivastava et al., 2022).

Taking the evidence was indicated that natural products and their active phytoconstituents had antiviral activity. It was summarised that *Moringa oleifera* had a potential effect against different SARS-CoV-2 protein and it helps to develop new compounds against coronaviruses and other viral species. The present study aimed to determine the effect of different active phytoconstituents of *Moringa oleifera* with different viral

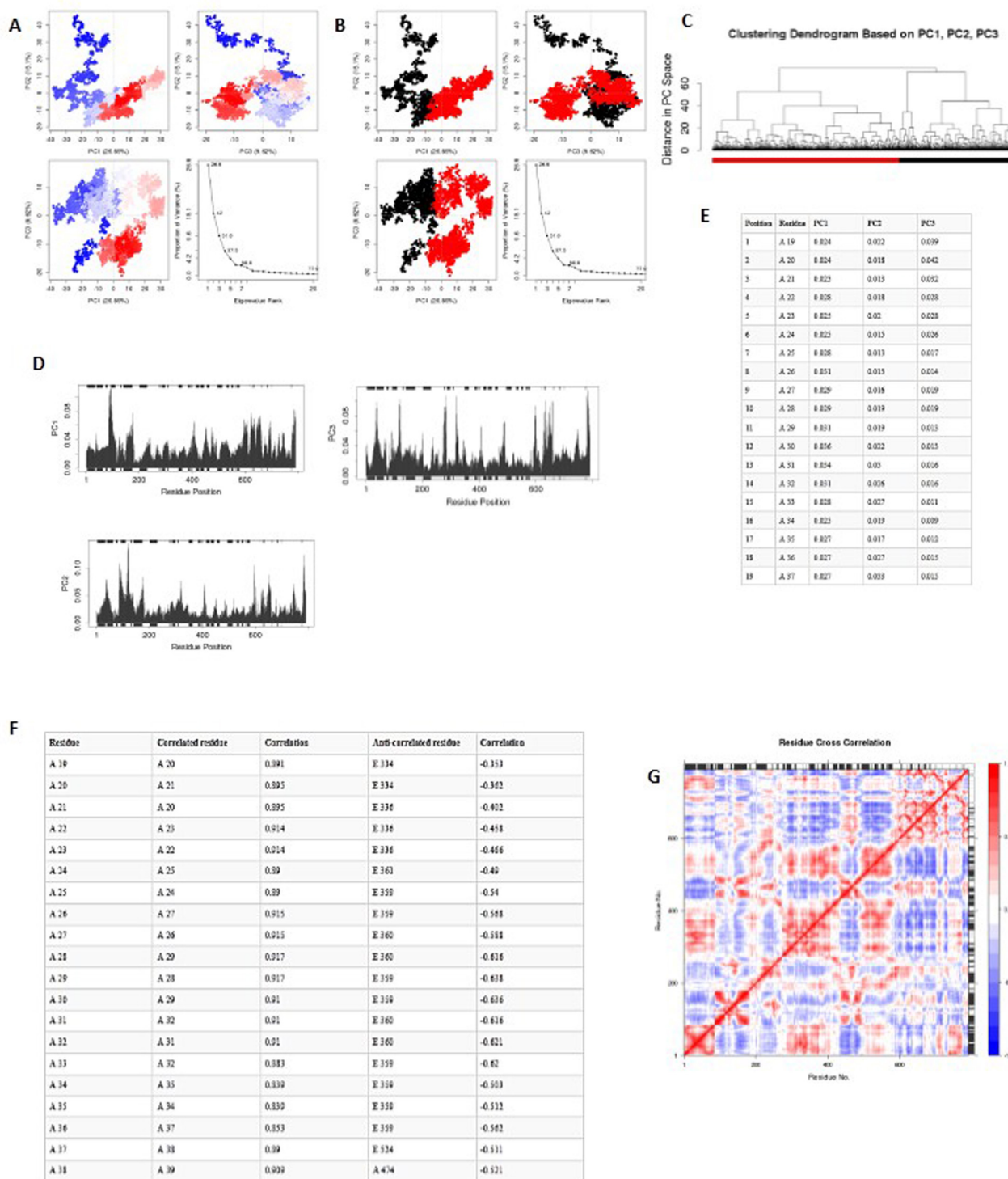


Figure 10. PCA of ACE-2 (PDB ID: 6MOJ) complexed with myricetin (A) PCA results for Trajectory (B) Simple clustering in PC subspace (C) Clustering dendrogram based on PC1, PC2, and PC3 (D) Residue-wise loadings for PC1, PC2 and PC3 (E) Table data showing residue-wise loadings for PC1, PC2 and PC3 and residue number at each position (F) Table showing pair-wise cross-correlation coefficients; higher correlated coefficient value is >0.8, and higher anti-correlated coefficient value is < 0.4 (G) Dynamical ResidueCross-correlation Map; the correlated residues are in blue, anti-correlated residues are in red; the pairwise residues with a higher correlated coefficient(>0.8) and with a higher anti-correlated coefficient (< 0.4) are linked with light pink and light blue (Int_mod).

A

ELE	VDW	GAS	PBSOL	PBTOT	GBSOL	GBTOT	TS	deltaPB	delatGB
-4.22	-41.20	-45.42	28.67	-16.74	16.23	-29.19	22.11	5.37	-7.08

C

Atyp1	Base1	Base2	Frames	Phi	Angle	Angle2
A:102-ADP602	1-12G:G99	1-12G:G91	1	8.990	14316	1217218
A:102-ADP60	1-12G:G99	1-12G:G94	1	8.998	8490	1217498
A:171-ADP602	1-12G:G87	1-12G:G94	1	8.995	54076	1217212
A:102-ADP60	1-12G:G99	1-12G:G93	1	8.999	29928	1217212
A:101-ADP60	1-12G:G99	1-12G:G91	2	8.998	8480	1216918
A:101-ADP60	1-12G:G99	1-12G:G93	2	8.995	14304	1216918
A:171-ADP602	1-12G:G87	1-12G:G94	2	8.995	11041	1217428
A:102-ADP60	1-12G:G99	1-12G:G94	2	8.992	8488	1217308
A:101-ADP602	1-12G:G99	1-12G:G94	3	8.998	12440	1217118
A:102-ADP60	1-12G:G99	1-12G:G93	3	8.992	11038	1216228
A:101-ADP604	1-12G:G99	1-12G:G91	4	8.994	8484	1217118
A:171-ADP60	1-12G:G87	1-12G:G91	4	8.983	5593	1216908
A:102-ADP60	1-12G:G99	1-12G:G93	4	8.984	11039	1216438
A:171-ADP602	1-12G:G99	1-12G:G93	5	8.985	11040	1216128
A:101-ADP602	1-12G:G99	1-12G:G91	6	8.998	8488	1216918
A:102-ADP602	1-12G:G99	1-12G:G91	6	8.995	11038	1216908
A:102-ADP602	1-12G:G99	1-12G:G94	8	8.999	8488	1216918
A:101-ADP602	1-12G:G99	1-12G:G91	8	8.998	11041	1216918
A:101-ADP60	1-12G:G97	1-12G:G94	8	8.998	8473	1216838
A:101-ADP604	1-12G:G95	1-12G:G94	10	8.999	5483	1216918
A:102-ADP602	1-12G:G99	1-12G:G94	17	8.992	12487	1216908
A:101-ADP602	1-12G:G99	1-12G:G94	20	8.997	8480	1216908
A:101-ADP60	1-12G:G99	1-12G:G94	9	8.987	8484	1216908
A:171-ADP604	1-12G:G99	1-12G:G94	16	8.973	11039	1216908
A:101-ADP60	1-12G:G97	1-12G:G96	40	8.979	12482	1216918
A:101-ADP602	1-12G:G99	1-12G:G94	42	8.978	12381	1216908
A:101-ADP60	1-12G:G97	1-12G:G96	47	8.972	12484	1216918
A:101-ADP602	1-12G:G99	1-12G:G96	54	8.974	12484	1216918
A:101-ADP604	1-12G:G99	1-12G:G91	55	8.983	8476	1216908
A:101-ADP602	1-12G:G99	1-12G:G91	56	8.989	8488	1216908
A:101-ADP60	1-12G:G99	1-12G:G94	59	8.989	8488	1216908
A:101-ADP60	1-12G:G99	1-12G:G94	125	8.987	12483	1216918
A:101-ADP602	1-12G:G97	1-12G:G96	170	8.974	12381	1216918
A:101-ADP60	1-12G:G97	1-12G:G96	181	8.986	12481	1216918
A:101-ADP602	1-12G:G99	1-12G:G96	246	8.976	12483	1216918
A:101-ADP602	1-12G:G99	1-12G:G96	248	8.970	12481	1216918
A:101-ADP60	1-12G:G99	1-12G:G91	88	8.989	8472	1216908
A:101-ADP602	1-12G:G99	1-12G:G94	140	8.976	12488	1216918
1-12G:G96	A:171-ADP602	A:171-ADP602	1	8.985	14011	1217448
1-12G:G97	A:171-ADP602	A:171-ADP602	1	8.982	14011	1217448
1-12G:G96	A:101-ADP60	A:101-ADP60	1	8.985	11039	1216908
1-12G:G95	A:101-ADP602	A:101-ADP602	1	8.985	11039	1216908
1-12G:G95	A:101-ADP602	A:101-ADP602	1	8.985	11039	1216908
1-12G:G95	A:101-ADP602	A:101-ADP602	2	8.989	11039	1216908
1-12G:G94	A:101-ADP602	A:101-ADP602	3	8.983	8472	1217122
1-12G:G91	A:101-ADP602	A:101-ADP602	3	8.983	8476	1216908
1-12G:G91	A:101-ADP602	A:101-ADP602	4	8.983	8476	1216908
1-12G:G91	A:101-ADP602	A:101-ADP602	3	8.983	8476	1216908
1-12G:G91	A:101-ADP602	A:101-ADP602	12	8.989	8476	1216918

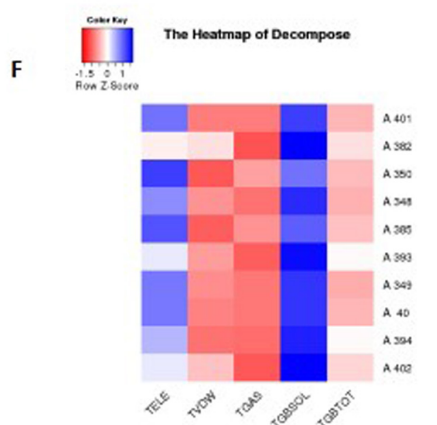
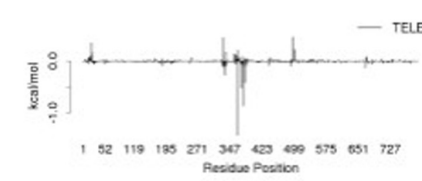
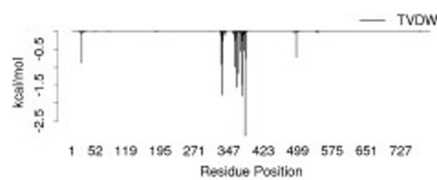
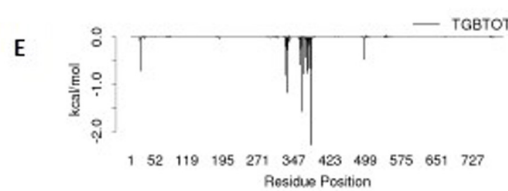
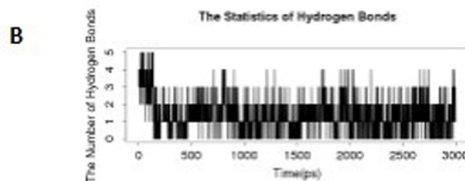


Figure 11. Energy, hydrogen bond analysis and decomposition analysis of ACE-2 protein (PDB ID:6MOJ) complexed with myricetin (A) MM/PB(G) SA result consists of electrostatic energy (ELE), van der Waals contribution (vDW), total gas-phase energy (GAS),non-polar and polar contributions to solvation (PBSOL/GBSOL) (B, C) Statistics of hydrogen bonds (D) Energy decompose of protein-ligand complex (kcal/mol) (E) Graphical representation of decompose result (F) Heatmap of decompose.

proteins of SARS-CoV-2 for the prevention of its replication into the host cell. Also, determine some active compounds were effectively bound to the SARS-CoV-2 viral proteins and show the greatest binding potential. The active constituents such as beta carotene and myricetin shows the best result as compared to other ligands and hydroxychloroquine used as a reference drug. These two compounds significantly formed a complex with all viral proteins. Similarly, with a comparison of beta carotene and myricetin, the beta carotene binding energy was better than myricetin. Still, the interacting amino acid and hydrogen bond formation is more in myricetin.

4. CONCLUSION

The *In Silico* study showed that all these active constituents had an excellent effect against SARS-CoV-2 viral proteins, mostly beta carotene and Myricetin. Several phytoconstituents with spike glycoproteins of SARS-CoV-2 showed a good binding affinity with beta carotene (BE -7.27 kd= 4.72 μ M and BE -4.07 kd=1.05 mM, squalene BE -8.42 kd=677.84 nM and BE -4.04 kd=1.3 mM similarly with vitamin E, BE -8.87 kd=314.99 nM and -8.34 kd 765.09 nM. These ligands with other proteins had the least interaction compared with spike glycoproteins. The beta carotene with the main protease had strong interaction BE -8.09 kd 1.18 nM, and beta carotene with helicase also showed good interaction, was BE -9.53 kd= 102.91. These findings strongly itemized that few ligands had broad-spectrum activity with different SARS-CoV-2 viral proteins with equal binding affinity; thus, the result was further validated through MD simulation analysis. The RMSD value of all three ligand and protein complexes showed the least deviation for 0.25 to 1.5 Å. This deviation indicated that the ligand was tightly bound with active protein sites. The 3ns Int_mod simulation revealed that these complexes showed stability at 300K temperature. The Q (x) of the present study showed 99% stability throughout the MD simulation whereas the PCA analysis confirms that (>0.8) valued of overlapping free folded atoms had good stability with all complexes. This study concluded that a few compounds of *Moringa oleifera* like vitamin E, beta carotene, and myricetin showed promising effects against SARS-CoV-2 viral proteins, and it is effective in COVID-19 infection.

CONFLICTS OF INTEREST

Authors declares no conflict of interest.

ACKNOWLEDGMENTS

We would like to acknowledge the principle of Universal College of Medical Sciences who provide the facility for this work.

ORCID

Amit Kumar Shrivastava	0000-0002-8915-9186
Dipendra Chaudhary	0000-0002-9547-6305
Laxmi Shrestha	0000-0002-2489-4278
Anjan Palikhey	0000-0002-0224-0791
Chandrajeet Kumar Yaadav	0000-0002-5979-1770
Deepak Basyal	0000-0003-4314-4728
Bishal Joshi	0000-0001-9096-4660
Mohammad Ujair Shekh	0000-0003-4911-4378

A. APPENDIX. SUPPLEMENTARY INFORMATION

Supplementary data to this article can be found online at <https://doi.org/10.53365/nrfhh/153401>.

AUTHOR CONTRIBUTIONS

Amit Kumar Shrivastava and Dipendra Chaudhary actively involved for conceptualization, data analysis, writing original draft. Laxmi Shrestha, Anjan Palikhey, Chandrajeet Kumar Yadav, Deepak Basyal, Bishal Joshi and Mohammad Ujair Shekh also help for writing the original draft and review and editing of the manuscript.

REFERENCES

- Ahmad, R., 2019. Steroidal glycoalkaloids from *Solanum nigrum* target cytoskeletal proteins: an in silico analysis. *PeerJ*. 3(7), 1–39. <https://doi.org/10.7717/peerj.6012>
- Alegbeleye, O.O., 2018. How functional is *Moringa oleifera*? A review of its nutritive, medicinal, and socioeconomic potential. *Food and Nutrition Bulletin*. 39, 149–170. <https://doi.org/10.1177/0379572117749814>
- Amabye, T.G., Tadesse, F.M., 2016. Phytochemical and Antibacterial Activity of *Moringa Oleifera* Available in the Market of Mekelle. *Journal of Analytical & Pharmaceutical Research*. 2(1), 1–4. <https://doi.org/10.15406/japlr.2016.02.00011>
- Ang, L., Song, E., Lee, H.W., Lee, M.S., 2020. Herbal Medicine for the Treatment of Coronavirus Disease 2019 (COVID-19): A Systematic Review and Meta-Analysis of Randomized Controlled Trials. *Journal of Clinical Medicine*. 9(5), 1–20. <https://doi.org/10.3390/jcm9051583>
- Aniyery, R.B., Sharma, A., Gupta, A., 2015. Molecular docking studies and in silico pharmacokinetic property study of synthesized organotin complex of (1r, 2s, 5r)-2-isopropyl-5-methylcyclohexanol. *Journal of Chemical and Pharmaceutical Sciences*. 9(4), 2656–2663.
- Belhassan, A., Chaita, S., Zaki, H., Alaqarbeh, M., Alsakhen, N., Almohtaseb, F., Lakhliifi, T., Bouachrine, M.J.J., 2022. In silico detection of potential inhibitors from vitamins and their derivatives compounds against SARS-CoV-2 main protease by using molecular docking, molecular dynamic simulation and ADMET profiling. *Journal of Molecular Structure*. 1258, 1–16. <https://doi.org/10.1016/j.molstruc.2022.132652>
- Brenk, R., Schipani, A., James, D., Krasowski, A., Gilbert, I.H., Frearson, J., Wyatt, P.G., 2008. Lessons learnt from assembling screening libraries for drug discovery for neglected diseases. *ChemMedChem*. 3(3), 435–444. <https://doi.org/10.1002/cmdc.200700139>

- Contreras-Puentes, N., Alviz-Amador, A., 2020. Virtual screening of natural metabolites and antiviral drugs with potential inhibitory activity against 3CL-PRO and PL-PRO. *Biomedical and Pharmacology Journal*. 13(2), 933–941. <https://dx.doi.org/10.13005/bpj/1962>
- Das, N., Sikder, K., Ghosh, S., Fromenty, B., Dey, S., 2012. *Moringa oleifera* Lam. leaf extract prevents early liver injury and restores antioxidant status in mice fed with high-fat diet. *Indian Journal of Experimental Biology*. 50, 404–412.
- Dolinsky, T.J., Czodrowski, P., Li, H., Nielsen, J.E., Jensen, J.H., Klebe, G., Baker, N.A., 2007. PDB2PQR: expanding and upgrading automated preparation of biomolecular structures for molecular simulations. *Nucleic acids research*. 35(Suppl_2), 522–525. <https://doi.org/10.1093/nar/gkm276>
- Du, L., He, Y., Zhou, Y., Liu, S., Zheng, B.J., Jiang, S., 2009. The spike protein of SARS-CoV-a target for vaccine and therapeutic development. *Nature Reviews Microbiology*. 7(3), 226–236. <https://doi.org/10.1038/nrmicro2090>
- Egan, W.J., Merz, K.M., Baldwin, J.J., 2000. Prediction of drug absorption using multivariate statistics. *Journal of Medicinal Chemistry*. 43(21), 3867–3877. <https://doi.org/10.1021/jm000292e>
- Ertl, P., Schuffenhauer, A., 2009. Estimation of synthetic accessibility score of drug-like molecules based on molecular complexity and fragment contributions. *Journal of Cheminformatics*. 1, 1–11. <https://doi.org/10.1186/1758-2946-1-8>
- Faber, M.S., Jetter, A., Fuhr, U., 2005. Assessment of CYP1A2 activity in clinical practice: why, how, and when? . *Basic & Clinical pharmacology & Toxicology*. 97, 125–134. https://doi.org/10.1111/j.1742-7843.2005.pto_973160.x
- Fang, S.H., Hou, Y.C., Chang, W.C., Hsiu, S.L., Chao, P.-D.L., Chiang, B.L., 2003. Morin sulfates/glucuronides exert anti-inflammatory activity on activated macrophages and decreased the incidence of septic shock. *Life Sciences*. 74(6), 743–756. <https://doi.org/10.1016/j.lfs.2003.07.017>
- Feng, Y., Wang, Q., Wang, T.J.B., 2017. Drug target protein-protein interaction networks: a systematic perspective. *BioMed Research International*. 2017, 1–14. <https://doi.org/10.1155/2017/1289259>
- Ferriola, P.C., Cody, V., Middleton, E., 1989. Protein kinase C inhibition by plant flavonoids: kinetic mechanisms and structure-activity relationships. *Biochemical Pharmacology*. 38(10), 1617–1624. [https://doi.org/10.1016/0006-2952\(89\)90309-2](https://doi.org/10.1016/0006-2952(89)90309-2)
- Franova, S., Kazimierova, I., Pappova, L., Joskova, M., Plank, L., Sutovska, M., 2016. Bronchodilatory, antitussive and anti-inflammatory effect of morin in the setting of experimentally induced allergic asthma. *Journal of Pharmacy and Pharmacology*. 68(8), 1064–1072. <https://doi.org/10.1111/jphp.12576>
- Ghose, A.K., Viswanadhan, V.N., Wendoloski, J.J., 1999. A knowledge-based approach in designing combinatorial or medicinal chemistry libraries for drug discovery. 1. A qualitative and quantitative characterization of known drug databases. *Journal of Combinatorial Chemistry*. 1(1), 55–68. <https://doi.org/10.1021/cc9800071>
- Gopalakrishnan, L., Doriya, K., Kumar, D.S., 2016. *Moringa oleifera*: A review on nutritive importance and its medicinal application. *Food Science and Human Wellness*. 5, 49–56. <https://doi.org/10.1016/j.fshw.2016.04.001>
- Gupta, A., Ahmad, R., Siddiqui, S., Yadav, K., Srivastava, A., Trivedi, A., Ahmad, B., Khan, M.A., Shrivastava, A.K., Singh, G.K., 2021. Flavonol morin targets host ACE2, IMP- α , PARP-1 and viral proteins of SARS-CoV-2, SARS-CoV and MERS-CoV critical for infection and survival: a computational analysis. *Journal of Biomolecular Structure and Dynamics*. 19, 1–32. <https://doi.org/10.1080/07391102.2021.1871863>
- Hann, M.M., Keserü, G.M., 2012. Finding the sweet spot: the role of nature and nurture in medicinal chemistry. *Nature Reviews Drug Discovery*. 11, 355–365. <https://doi.org/10.1038/nrd3701>
- Harapan, H., Itoh, N., Yufika, A., Winardi, W., Keam, S., Te, H., Megawati, D., Hayati, Z., Wagner, A.L., Mudatsir, M., 2020. Coronavirus disease 2019 (COVID-19): A literature review. *Journal of Infection and Public Health*. 13(5), 667–673. <https://doi.org/10.1016/j.jiph.2020.03.019>
- Hospital, A., Goñi, J.R., Orozco, M., Gelpí, J.L., 2015. Molecular dynamics simulations: advances and applications. *Advances and applications in bioinformatics and chemistry: AABC*. 8, 37. <http://dx.doi.org/10.2147/AABC.S70333>
- Imran, I., Altaf, I., Ashraf, M., Javeed, A., Munir, N., Bashir, R., 2016. In vitro evaluation of antiviral activity of leaf extracts of *Azadirachta indica*, *Moringa oleifera*, and *Morus alba* against the foot and mouth disease virus on BHK-21 cell line. *ScienceAsia*. 42(6), 396–396. [10.2306/scienceasia1513-1874.2022.48.000](https://doi.org/10.2306/scienceasia1513-1874.2022.48.000)
- Kadri, A., Aouadi, K., 2020. In vitro antimicrobial and α -glucosidase inhibitory potential of enantiopure cycloalkylglycine derivatives: Insights into their in silico pharmacokinetic, druglikeness, and medicinal chemistry properties. *Journal of Applied Pharmaceutical Sciences*. 10, 107–115. <http://dx.doi.org/10.7324/JAPS.2020.10614>
- Kaiser, K.L., Valdmans, I., 1982. Apparent octanol/water partition coefficients of pentachlorophenol as a function of pH. *Canadian Journal of Chemistry*. 60(16), 2104–2106. <https://doi.org/10.1139/v82-300>
- Khan, T., Azad, I., Ahmad, R., Raza, S., Dixit, S., Joshi, S., Khan, A.R., 2018. Synthesis, characterization, computational studies and biological activity evaluation of Cu, Fe, Co and Zn complexes with 2-butanone thiosemicarbazone and 1, 10-phenanthroline ligands as anticancer and antibacterial agents. *EXCLI Journal*. 17, 331–348. <https://doi.org/10.17179/excli2017-984>
- Kumar, T.A., Kabilan, S., Parthasarathy, V., 2017. Screening and Toxicity Risk Assessment of Selected Compounds to Target Cancer using QSAR and Pharmacophore Modelling. *International Journal of Pharm Tech Research*. 10, 219–224. <http://dx.doi.org/10.20902/IJPTR.2017.10428>
- Li, Y., Liu, X.Z., You, Z.H., Li, L.P., Guo, J.X., Wang, Z.J.I.J.O.I.S., 2021. A computational approach for predicting drug-target interactions from protein sequence and drug substructure fingerprint information. *International Journal of Intelligent System*. 36(1), 593–609. <https://doi.org/10.1002/int.22332>
- Linani, A., Benarous, K., Bou-Salah, L., Yousfi, M., Goumri-Said, S.J.I.J.O.P.R., Therapeutics., 2022. Exploring Structural Mechanism of COVID-19 Treatment with Glutathione as a Potential Peptide Inhibitor to the Main Protease: Molecular Dynamics Simulation and MM/PBSA Free Energy Calculations Study. *International Journal of Peptide Research and Therapeutics*. 28(55), 1–16. <https://doi.org/10.1007/s10989-022-10365-6>
- Lipinski, C.A., Lombardo, F., Dominy, B.W., Feeney, P.J., 1997. Experimental and computational approaches to estimate solubility and permeability in drug discovery and development settings. *Advanced Drug Delivery Reviews*. 23, 423–424. [https://doi.org/10.1016/S0169-409X\(96\)00423-1](https://doi.org/10.1016/S0169-409X(96)00423-1)
- Martin, Y.C., 2005. A bioavailability score. *Journal of Medicinal Chemistry*. 48(9), 3164–3170. <https://doi.org/10.1021/jm0492002>
- Meanwell, N.A., 2016. Improving drug design: an update on recent applications of efficiency metrics, strategies for replacing problematic elements, and compounds in nontraditional drug space. *Chemical Research in Toxicology*. 29(4), 564–616. <https://doi.org/10.1021/acs.chemrestox.6b00043>
- Muegge, I., Heald, S.L., Brittelli, D., 2001. Simple selection criteria for drug-like chemical matter. *Journal of Medicinal Chemistry*. 44(12),

- 1841–1846. <https://doi.org/10.1021/jm015507e>
- Murgolo, N., Therien, A.G., Howell, B., Klein, D., Koeplinger, K., Lieberman, L.A., Adam, G.C., Flynn, J., Mckenna, P., Swaminathan, G., 2021. SARS-CoV-2 tropism, entry, replication, and propagation: Considerations for drug discovery and development. *PLoS Pathogens*. 17(2), 1–18. <https://doi.org/10.1371/journal.ppat.1009225>
- Nair, A., James, T., 2020. Computational screening of phytochemicals from *Moringa oleifera* leaf as potential inhibitors of SARS-CoV-2 Mpro. Preprint Research Square, 1–14. <https://doi.org/10.21203/rs.3.rs-71018/v1>
- Ni, W., Yang, X., Yang, D., Bao, J., Li, R., Xiao, Y., Hou, C., Wang, H., Liu, J., Yang, D., 2020. Role of angiotensin-converting enzyme 2 (ACE2) in COVID-19. *Critical Care*. 24, 1–10. <https://doi.org/10.1186/s13054-020-03120-0>
- Nworu, C., Okoye, E., Ezeifeka, G., Esimone, C., 2013. Extracts of *Moringa oleifera* Lam. showing inhibitory activity against early steps in the infectivity of HIV-1 lentiviral particles in a viral vector-based screening. *African Journal of Biotechnology*. 12(30), 1–8. <https://doi.org/10.5897/AJB2013.12343>
- Panyod, S., Ho, C.T., Sheen, L.Y., 2020. Dietary therapy and herbal medicine for COVID-19 prevention: A review and perspective. *Journal of Traditional and Complementary Medicine*. 10(4), 420–427. <https://doi.org/10.1016/j.jtcme.2020.05.004>
- Petit, L., Vernès, L., Cadoret, J.P., 2021. Docking and in silico toxicity assessment of Arthrospira compounds as potential antiviral agents against SARS-CoV-2. *Journal of Applied Phycology*. 33(3), 1579–1602. <https://doi.org/10.1007/s10811-021-02372-9>
- Siddiqui, S., Upadhyay, S., Ahmad, R., Gupta, A., Srivastava, A., Trivedi, A., Husain, I., Ahmad, B., Ahamed, M., Khan, M.A., 2022. Virtual screening of phytoconstituents from miracle herb *Nigella sativa* targeting nucleocapsid protein and papain-like protease of SARS-CoV-2 for COVID-19 treatment. *Journal of Biomolecular Structure and Dynamics*. 40(9), 3928–3948. <https://doi.org/10.1080/07391102.2020.1852117>
- Sisakht, M., Mahmoodzadeh, A., Darabian, M., 2021. Plant-derived chemicals as potential inhibitors of SARS-CoV-2 main protease (6LU7), a virtual screening study. *Phytotherapy Research*. 35(6), 3262–3274. <https://doi.org/10.1002/ptr.7041>
- Srivastava, A., Siddiqui, S., Ahmad, R., Mehrotra, S., Ahmad, B., Srivastava, A., 2022. Exploring nature's bounty: identification of *Withania somnifera* as a promising source of therapeutic agents against COVID-19 by virtual screening and in silico evaluation. *Journal of Biomolecular Structure and Dynamics*. 40(4), 1858–1908. <https://doi.org/10.1080/07391102.2020.1835725>
- Tallei, T.E., Tumilaar, S.G., Niode, N.J., Kepel, B.J., Idroes, R., Effendi, Y., Sakib, S.A., Emran, T.B., 2020. Potential of plant bioactive compounds as SARS-CoV-2 main protease (Mpro) and spike (S) glycoprotein inhibitors: a molecular docking study. *Scientifica*. 2020, 1–18. <https://doi.org/10.1155/2020/6307457>
- Teague, S.J., Davis, A.M., Leeson, P.D., Oprea, T., 1999. The design of leadlike combinatorial libraries. *Angewandte Chemie International Edition*. 38(24), 3743–3748. [https://doi.org/10.1002/\(SICI\)15213773\(19991216\)38:24<3743::AID-ANIE3743>3.0.CO;2-U](https://doi.org/10.1002/(SICI)15213773(19991216)38:24<3743::AID-ANIE3743>3.0.CO;2-U)
- Thapa, K., Poudel, M., Adhikari, P., 2019. *Moringa oleifera*: a review article on nutritional properties and its prospect in the context of Nepal. *Acta Scientific Agriculture*. 3, 47–54. <http://dx.doi.org/10.31080/ASAG.2019.03.0683>
- Touret, F., De Lamballerie, X., 2020. Of chloroquine and COVID-19. *Antiviral Research*. 177, 1–2. <https://doi.org/10.1016/j.antiviral.2020.104762>
- Trivedi, A., Ahmad, R., Siddiqui, S., Misra, A., Khan, M.A., Srivastava, A., Ahamad, T., Khan, M.F., Siddiqui, Z., Afrin, G., 2021. Prophylactic and therapeutic potential of selected immunomodulatory agents from Ayurveda against coronaviruses amidst the current formidable scenario: an in silico analysis. *Journal of Biomolecular Structure and Dynamics*, 1–53. <https://doi.org/10.1080/07391102.2021.1932601>
- Ursu, O., Rayan, A., Goldblum, A., Oprea, T.I., 2011. Understanding drug-likeness. *Wiley Interdisciplinary Reviews: Computational Molecular Science*. 1, 760–781. <https://doi.org/10.1002/wcms.52>
- Veber, D.F., Johnson, S.R., Cheng, H.Y., Smith, B.R., Ward, K.W., Kopple, K.D., 2002. Molecular properties that influence the oral bioavailability of drug candidates. *Journal of Medicinal Chemistry*. 45(12), 2615–2623. <https://doi.org/10.1021/jm020017n>
- Verma, A., 2012. Lead finding from *Phyllanthus debelis* with hepatoprotective potentials. *Asian Pacific Journal of Tropical Biomedicine*. 2(12), 60486–60495. [https://doi.org/10.1016/S2221-1691\(12\)60486-9](https://doi.org/10.1016/S2221-1691(12)60486-9)
- Yang, J., Zheng, Y., Gou, X., Pu, K., Chen, Z., Guo, Q., Ji, R., Wang, H., Wang, Y., Zhou, Y., 2020. Prevalence of comorbidities and its effects in patients infected with SARS-CoV-2: a systematic review and meta-analysis. *International Journal of Infectious Diseases*. 94, 91–95. <https://doi.org/10.1016/j.ijid.2020.03.017>